Trends in Glycoscience and Glycotechnology
Vol.17 No.97 (September 2005) pp.193–203

glycopeptides, including a single glycosylation site. Trypsin, Lys-C, Glu-C and Asp-N are commonly used for glycosylation analysis. Since glycopeptide ions are sometimes missed by MS in the presence of excess peptides due to their lower ionization efficiency, several methods have been proposed for the fractionation of glycopeptides, such as HPLC and affinity chromatography (57,58), followed by off-line MALDI-MS. LC on-line ESI/MS is an efficient method for the direct elucidation of glycopeptides in a complex mixture. Although LC/MS provide a complicated chromatogram, glycopeptides in a choromatographic position can be localized by the appearance of marker ions, such as $HexNAc^+$ and $HexHexNAc^+$, resulting from precursor ion scanning and in-source CID (59–66). However, for peptide identification these two means require additional CID-MS/MS scan for some intense ions (data-dependent CID-MS/MS scan). Recently we presented an alternative method, with which product ion spectra of glycopeptides can be selected directly using marker ions arising from glycopeptides by data-dependent CID-MS/MS scan with relatively high energy (49).

める。まず、糖タンパク質を適切な酵素で糖ペプチドに断片化する。この際、同一ペプチドに複数の糖鎖結合部位が含まれないように酵素を選択する。基質特異性の高いトリプシン、Lys-C、Glu-C、及びAsp-N等がよく用いられている。糖ペプチドはペプチドに比べてイオン化効率が悪く、ペプチドが混在するとマススペクトルが得られにくい。そのため、アフィニティークロマトグラフィーや、HPLC等で予め糖ペプチドを分画してから(57、58)、マススペクトルを測定するオフライン法(図7A)や、C18カラム等を用いたLC/MSでペプチド・糖ペプチドを分離しながら直接マススペクトルを測定するオンライン法がよく用いられている(図7B)。オンラインLC/MSでは複雑なクロマトグラムが得られるが、プリカーサーイオンスキャンやインソースCIDによって生じた糖鎖に特徴的なBイオン(例えば、$HexNAc^+$、*m/z* 204や$HexHexNAc^+$、*m/z* 366など)を利用することによって、糖ペプチドの溶出位置を推定することができる(59–66)。ただしこれらの方法は、ペプチドを同定するために、別途、強度の高いイオンに対する自動的CID-MS/MSスキャン(データ依存的CID-MS/MSスキャン)を行う必要がある。そこで、我々は別法として、データ依存的なCID-MS/MSによって生成したBイオンを利用して糖ペ

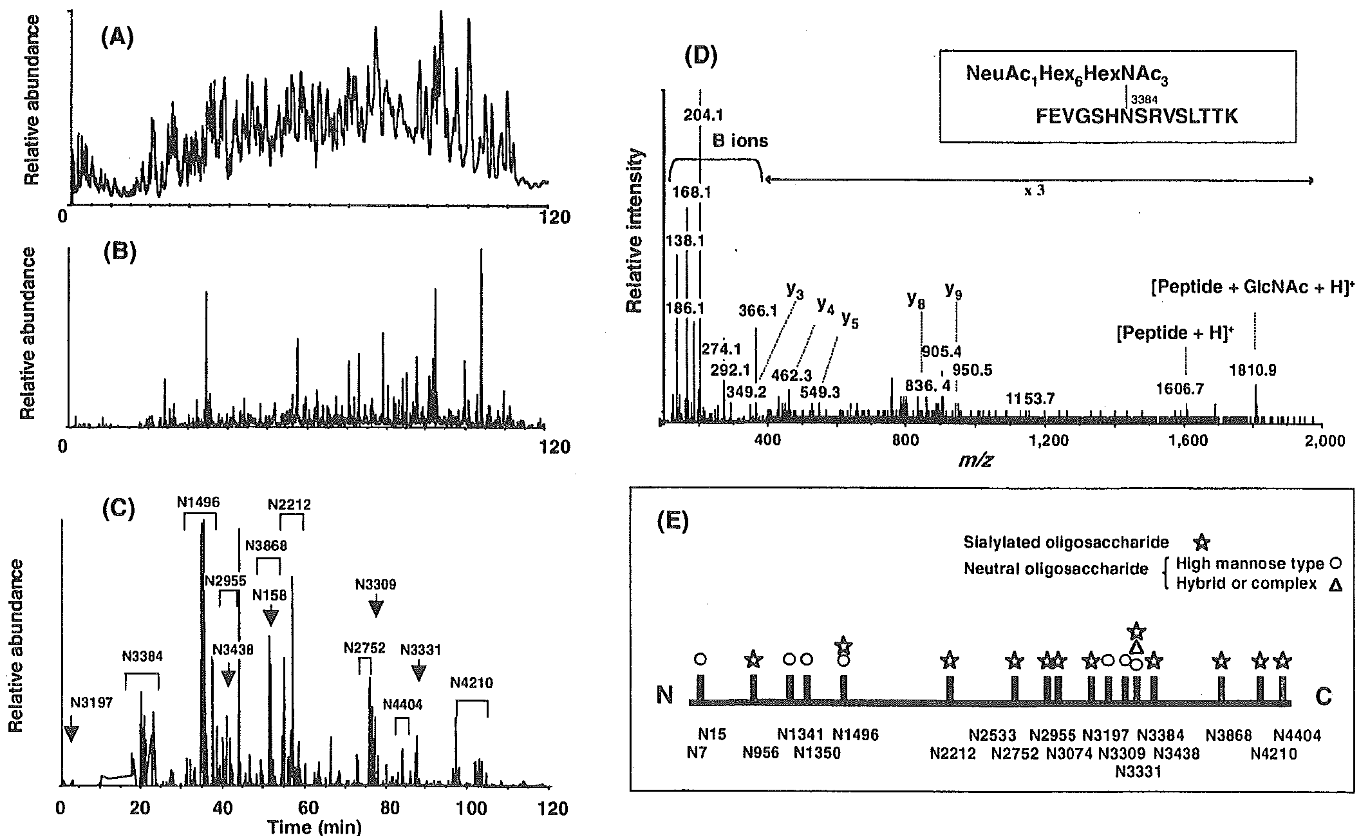


**Fig. 8. Site-specific glycosylation analysis of apoB100 by LC/ESI-MS/MS.** (A) TIC of full MS scan (*m/z* 400-2,000). (B) TIC of data-dependent CID-MS/MS scan (*m/z* 100-2,000). (C) Mass chromatogram at *m/z* 204 in data-dependent CID-MS/MS scan. (D) MS/MS spectrum of glycopeptide (precursor ion: *m/z* 1,160.4). (E) *N*-glycosylation of apoB100. Sample: tryptic digest of apoB100 (4 μg), LC: Paradigm (Michrome BioResources), Column: Magic C18 (0.2 × 50 mm, Michrome BioResources), MS: QSTAR (Applied Biosystems).


©2005 FCCA (Forum: Carbohydrates Coming of Age)

Trends in Glycoscience and Glycotechnology
Vol.17 No.97 (September 2005) pp.193–203

Here we demonstrate the site-specific glycosylation analysis of human apolipoprotein B100 (apoB100). Tryptic digest of apoB (4 μg) was injected into an LC/ESI-QqTOFMS instrument equipped with a C18 column. Figs. 8A and B are total ion chromatograms (TIC) obtained by full $MS^1$ scan and data-dependent CID-MS/MS scan, respectively (49). These chromatograms appear complicated due to a number of peptide-related ions derived from a large glycoprotein molecule of 500,000 Da. In order to localize glycopeptides in the peptide map, carbohydrate marker ion, $HexNAc^+$ at *m/z* 204, was extracted from the TIC of data-dependent CID-MS/MS scan (Fig. 8C). The MS/MS spectra of glycopeptides were then sorted from the peaks appearing in the mass chromatogram (Fig. 8D). We successfully identified 17 *N*-glycosylation sites among 19 potential *N*-glycosylation sites and deduced glycosylation at each glycosylation site from the mass of carbohydrate moieties (Fig. 8E).

プチドのMS/MSスペクトルを選び出す方法を見出した(49)。

図8に、我々が最近行ったオンライン法によるヒトアポリポプロテインB100 (apoB100)の部位特異的な糖鎖解析例を示す(49)。apoB100のトリプシン消化物(4 μg)をC18カラムを用いたLC/ESI-QqTOFMS装置で分析した。図8A及びBはフル$MS^1$スキャン(*m/z* 1,000-2,000)及びデータ依存的CID-MS/MSスキャンによって得られたトータルイオンクロマトグラム(TIC)である。apoB100は分子量約500,000 Daの大きな糖タンパク質なので、非常に多くのペプチドイオンが検出されている。そこで、糖ペプチドの溶出位置を推定するために、データ依存的CID-MS/MSスキャンによって生じた*m/z* 204イオンのみを抜き出した(図8C)。出現したピーク周辺からBイオンを指標に糖ペプチドのMS/MSスペクトルを探し出し、それらのスペクトル上のプロダクトイオンを帰属した(図8D)。その結果、19カ所の推定*N*結合型糖鎖結合部位のうち17カ所に糖鎖が結合していることを明らかにするとともに、それぞれの部位に結合している糖鎖を推定することができた(図8E)。

## F. Application in Proteomics and Glycomics

MS enables us to elucidate a small number of glycoproteins isolated by electrophoresis (67, 68) and micro HPLC (69). This method could be applied in comprehensive or carbohydrate structure-specific glycoprotein analysis by a combination with proteomic approaches such as 2-dimensional (2D) gel electrophoresis (GE) and 2D-LC followed by MS. Some applications have been already demonstrated, for instance, glycoprotein expression analysis using 2D-GE coupled with carbohydrate-specific dyeing or immunoblotting (70), and LC/MS combined with lectin affinity chromatography (71,72). These glycomic/proteomic technologies are expected to be a powerful tool for the functional study of glycoproteins, finding disease-related glycoproteins and identifying proteins attached to some glyco-epitopes.

## F. グライコミクス・プロテオミクスへの応用

現在では、電気泳動(67、68)やミクロ液体クロマトグラフィー(69)で分離された僅かな糖タンパク質からでも、MSによって、多くの糖鎖構造情報を得ることができるようになった。これらの糖鎖解析技術とプロテオミクス的アプローチ、すなわち、2次元電気泳動や2次元クロマトグラフィーによるタンパク質発現解析とMSを組み合わせることによって、糖タンパク質の網羅的解析や、任意の糖鎖構造を持つタンパク質の解析が可能になるものと期待されている。すでに、2次元電気泳動と糖タンパク質特異的染色法や免疫ブロットを組み合わせた糖タンパク質発現解析や(70)、レクチンアフィニティークロマトグラフィーと各種LC/MSを組み合わせた糖タンパク質の網羅的解析の例が報告されている(71、72)。今後、これらのグライコミクス・プロテオミクス解析技術が、糖鎖の機能研究や、疾患等に関与する糖鎖・糖タンパク質の探索、並びに様々な糖鎖エピトープ結合タンパク質の特定に貢献できるものと期待される。

## References

1. Karas, M., and Hillenkamp, F. (1988) Anal. Chem. **60**, 2299–2301
2. Fenn, J. B., Mann, M., Meng, C. K., Wong, S. F., and Whitehouse, C. M. (1989) Science **246**, 64–71
3. Lemoine, J., Chirat, F., and Domon, B. (1996) J. Mass Spectrom. **31**, 908–912
4. Bahr, U., Pfenninger, A., Karas, M., and Stahl, B. (1997) Anal. Chem. **69**, 4530–4535
5. Hunt, D. F., Yates, J. R., 3rd, Shabanowitz, J., Winston, S., and Hauer, C. R. (1986) Proc. Natl. Acad. Sci. U S A. **83**, 6233–6237
6. Weiskopf, A. S., Vouros, P., and Harvey, D. J. (1998) Anal. Chem. **70**, 4441–4447
7. Naven, T. J., Harvey, D. J., Brown, J., and Critchley, G. (1997) Rapid Commun. Mass Spectrom. **11**, 1681–1686
8. Solouki, T., Reinhold, B. B., Costello, C. E., O'Malley, M., Guan, S., and Marshall, A. G. (1998) Anal. Chem. **70**, 857–864
9. Chai, W., Piskarev, V., and Lawson, A. M. (2001) Anal. Chem. **73**, 651–657
10. Harvey, D. J., Bateman, R. H., Bordoli, R. S., and Tyldesley, R. (2000) Rapid Commun. Mass Spectrom. **14**, 2135–2142
11. Sagi, D., Peter-Katalinic, J., Conradt, H. S., and Nimtz, M. (2002) J. Am. Soc. Mass Spectrom. **13**, 1138–1148
12. Zhang, S., and Chelius, D. (2004) J. Biomol. Tech. **15**, 120–133
13. Karlsson, N. G., Schulz, B. L., and Packer, N. H. (2004) J. Am. Soc. Mass Spectrom. **15**, 659–672
14. Domon, B., and Costello, C. E. (1988) Glycoconj. J. **5**, 397–409
15. Meisen, I., Peter-Katalinic, J., and Muthing, J. (2003) Anal. Chem. **75**, 5719–5725
16. Xue, J., Song, L., Khaja, S. D., Locke, R. D., West, C. M., Laine, R. A., and Matta, K. L. (2004) Rapid Commun. Mass Spectrom. **18**, 1947–1955


©2005 FCCA (Forum: Carbohydrates Coming of Age)

Trends in Glycoscience and Glycotechnology
Vol.17 No.97 (September 2005) pp.193–203

17. Takegawa, Y., Deguchi, K., Ito, S., Yoshioka, S., Sano, A., Yoshinari, K., Kobayashi, K., Nakagawa, H., Monde, K., and Nishimura, S. (2004) Anal Chem. **76**, 7294–7303
18. Takegawa, Y., Deguchi, K., Ito, S., Yoshioka, S., Nakagawa, H., and Nishimura, S. (2005) Rapid Commun. Mass Spectrom. **19**, 937–946
19. Harvey, D. J. (1999) Mass Spectrom. Rev. **18**, 349–450
20. Harvey, D. J., Bateman, R. H., and Green, M. R. (1997) J. Mass Spectrom. **32**, 167–187
21. Kawasaki, N., Ohta, M., Hyuga, S., Hashimoto, O., and Hayakawa, T. (1999) Anal. Biochem. **269**, 297–303
22. Kawasaki, N., Haishima, Y., Ohta, M., Itoh, S., Hyuga, M., Hyuga, S., and Hayakawa, T. (2001) Glycobiology **11**, 1043–1049
23. Sato, Y., Suzuki, M., Nirasawa, T., Suzuki, A., and Endo, T. (2000) Anal. Chem. **72**, 1207–1216
24. Takegawa, Y., Deguchi, K., Ito, S., Yoshioka, S., Nakagawa, H., and Nishimura, S. (2005) Anal. Chem. **77**, 2097–2106
25. Royle, L., Mattu, T. S., Hart, E., Langridge, J. I., Merry, A. H., Murphy, N., Harvey, D. J., Dwek, R. A., and Rudd, P. M. (2002) Anal. Biochem. **304**, 70–90
26. Hase, S., Ikenaka, T., and Matsushima, Y. (1981) J. Biochem. (Tokyo). **90**, 407–414
27. Suzuki-Sawada, J., Umeda, Y., Kondo, A., and Kato, I. (1992) Anal. Biochem. **207**, 203–207
28. Bigge, J. C., Patel, T. P., Bruce, J. A., Goulding, P. N., Charles, S. M., and Parekh, R. B. (1995) Anal. Biochem. **230**, 229–238
29. Ohta, M., Hamako, J., Yamamoto, S., Hatta, H., Kim, M., Yamamoto, T., Oka, S., Mizuochi, T., and Matsuura, F. (1991) Glycoconj. J. **8**, 400–413
30. Yoshimi, Y., Yamazaki, S., and Ikekita, M. (1999) Biochem. Biophys. Acta. **1426**, 69–79
31. Suzuki, S., Kakehi, K., and Honda, S. (1996) Anal. Chem. **68**, 2073–2083
32. Okamoto, M., Takahashi, K., and Doi, T. (1995) Rapid Commun. Mass Spectrom. **9**, 641–643
33. Lattova, E., and Perreault, H. (2003) J. Chromatogr. A. **1016**, 71–87
34. Morelle, W., Faid, V., and Michalski, J. C. (2004) Rapid Commun. Mass Spectrom. **18**, 2451–2464
35. Yoshino, K., Takao, T., Murata, H., and Shimonishi, Y. (1995) Anal. Chem. **67**, 4028–4031
36. Kawasaki, N., Ohta, M., Itoh, S., Hyuga, M., Hyuga, S., and Hayakawa, T. (2002) Biologicals. **30**, 113–123
37. Karlsson, N. G., Wilson, N. L., Wirth, H. J., Dawes, P., Joshi, H., and Packer, N. H. (2004) Rapid Commun. Mass Spectrom. **18**, 2282–2292
38. Zamfir, A., Seidler, D. G., Schonherr, E., Kresse, H., and Peter-Katalinic, J. (2004) Electrophoresis **25**, 2010–2016
39. Kremmer, T., Szollosi, E., Boldizsar, M., Vincze, B., Ludanyi, K., Imre, T., Schlosser, G., and Vekey, K. (2004) Biomed. Chromatogr. **18**, 323–329
40. Hashii, N., Kawasaki, N., Itoh, S., Hyuga, M., Kawanishi, T., and Hayakawa, T. (2005) Proteomics (in press)
41. Yuan, J., Hashii, N., Kawasaki, N., Itoh, S., Kawanishi, T., and Hayakawa, T. (2005) J. Chromatogr. A. **1067**, 145–152
42. Demelbauer, U. M., Zehl, M., Plematl, A., Allmaier, G., and Rizzi, A. (2004) Rapid Commun. Mass Spectrom. **18**, 1575–1582
43. Roepstorff, P., and Fohlman, J. (1984) Biomed. Mass Spectrom. **11**, 601
44. Hakansson, K., Chalmers, M. J., Quinn, J. P., McFarland, M. A., Hendrickson, C. L., and Marshall, A. G. (2003) Anal. Chem. **75**, 3256–3262
45. Hakansson, K., Cooper, H. J., Emmett, M. R., Costello, C. E., Marshall, A. G., and Nilsson, C. L. (2001) Anal. Chem. **73**, 4530–4536
46. Kurogochi, M., and Nishimura, S. (2004) Anal. Chem. **76**, 6097–6101
47. Krokhin, O., Ens, W., Standing, K. G., Wilkins, J., and Perreault, H. (2004) Rapid Commun. Mass Spectrom. **18**, 2020–2030
48. Wuhrer, M., Hokke, C. H., and Deelder, A. M. (2004) Rapid Commun. Mass Spectrom. **18**, 1741–1748
49. Harazono, A., Kawasaki, N., Kawanishi, T., and Hayakawa, T. (2005) Glycobiology **15**, 447–462
50. Nemeth, J. F., Hochgesang, G. P., Jr., Marnett, L. J., and Caprioli, R. M. (2001) Biochemistry **40**, 3109–3116
51. Hui, J. P., White, T. C., and Thibault, P. (2002) Glycobiology **12**, 837–849
52. Sandra, K., Devreese, B., Van Beeumen, J., Stals, I., and Claeyssens, M. (2004) J. Am. Soc. Mass Spectrom. **15**, 413–423
53. Sandra, K., Stals, I., Sandra, P., Claeyssens, M., Van Beeumen, J., and Devreese, B. (2004) J. Chromatogr. A. **1058**, 263–272
54. Satomi, Y., Shimonishi, Y., and Takao, T. (2004) FEBS Lett. **576**, 51–56
55. Wada, Y., Tajiri, M., and Yoshida, S. (2004) Anal. Chem. **76**, 6560–6565
56. Itoh, S., Kawasaki, N., Hashii, N., Harazono, A., Matsuishi, Y., Kawanishi, T., and Hayakawa, T. (2005) J. Chromatogr. A. Submitted
57. Garcia, R., Rodriguez, R., Montesino, R., Besada, V., Gonzalez, J., and Cremata, J. A. (1995) Anal. Biochem. **231**, 342–348
58. Fu, D., and van Halbeek, H. (1992) Anal. Biochem. **206**, 53–63
59. Carr, S. A., Huddleston, M. J., and Bean, M. F. (1993) Protein Sci. **2**, 183–196
60. Ethier, M., Saba, J. A., Spearman, M., Krokhin, O., Butler, M., Ens, W., Standing, K. G., and Perreault, H. (2003) Rapid Commun. Mass Spectrom. **17**, 2713–2720
61. Huddleston, M. J., Bean, M. F., and Carr, S. A. (1993) Anal. Chem. **65**, 877–884
62. Kapron, J. T., Hilliard, G. M., Lakins, J. N., Tenniswood, M. P., West, K. A., Carr, S. A., and Crabb, J. W. (1997) Protein Sci. **6**, 2120–2133
63. Medzihradszky, K. F., Besman, M. J., and Burlingame, A. L. (1997) Anal. Chem. **69**, 3986–3994
64. Ritchie, M. A., Gill, A. C., Deery, M. J., and Lilley, K. (2002) J. Am. Soc. Mass Spectrom. **13**, 1065–1077
65. Schindler, P. A., Settineri, C. A., Collet, X., Fielding, C. J., and Burlingame, A. L. (1995) Protein Sci. **4**, 791–803
66. Wang, F., Nakouzi, A., Angeletti, R. H., and Casadevall, A. (2003) Anal. Biochem. **314**, 266–280
67. Wilson, N. L., Schulz, B. L., Karlsson, N. G., and Packer, N. H. (2002) J. Proteome Res. **1**, 521–529
68. Itoh, S., Harazono, A., Kawasaki, N., Hashii, N., Matsuishi, Y., Kawanishi, T., and Hayakawa, T. (2004) J. Electrophoresis **48**, 163–168
69. Fan, X., She, Y. M., Bagshaw, R. D., Callahan, J. W., Schachter, H., and Mahuran, D. J. (2004) Anal. Biochem. **332**, 178–186
70. Higai, K., Shibukawa, K., Muto, S., and Matsumoto, K. (2003) Anal. Sci. **19**, 85–92
71. Kaji, H., Saito, H., Yamauchi, Y., Shinkawa, T., Taoka, M., Hirabayashi, J., Kasai, K., Takahashi, N., and Isobe, T. (2003) Nat. Biotechnol. **21**, 667–672
72. Qiu, R., and Regnier, F. E. (2005) Anal. Chem. **77**, 2802–2809

*Received on June 3, 2005, accepted on July 19, 2005*



©2005 FCCA (Forum: Carbohydrates Coming of Age)

ELSEVIER

Available online at www.sciencedirect.com

SCIENCE DIRECT

Analytical Biochemistry 348 (2006) 259–268

ANALYTICAL BIOCHEMISTRY

www.elsevier.com/locate/yabio

# Site-specific N-glycosylation analysis of human plasma ceruloplasmin using liquid chromatography with electrospray ionization tandem mass spectrometry

Akira Harazono *, Nana Kawasaki, Satsuki Itoh, Noritaka Hashii, Akiko Ishii-Watabe, Toru Kawanishi, Takao Hayakawa

*National Institute of Health Sciences, Division of Biological Chemistry and Biologicals, 1-18-1 Kami-yoga, Setagaya-Ku, Tokyo 158-8501, Japan*

Received 8 June 2005
Available online 10 November 2005

**Abstract**

Ceruloplasmin has ferroxidase activity and plays an essential role in iron metabolism. In this study, a site-specific glycosylation analysis of human ceruloplasmin (CP) was carried out using reversed-phase high-performance liquid chromatography with electrospray ionization tandem mass spectrometry (LC-ESI-MS/MS). A tryptic digest of carboxymethylated CP was subjected to LC-ESI-MS/MS. Product ion spectra acquired data-dependently were used for both distinction of the glycopeptides from the peptides using the carbohydrate B-ions, such as *m/z* 204 (HexNAc) and *m/z* 366 (HexHexNAc), and identification of the peptide moiety of the glycopeptide based on the presence of the b- and y-series ions derived from the peptide. Oligosaccharide composition was deduced from the molecular weight calculated from the observed mass of the glycopeptide and theoretical mass of the peptide. Of the seven potential N-glycosylation sites, four (Asn119, Asn339, Asn378, and Asn743) were occupied by a sialylated biantennary or triantennary oligosaccharide with fucose residues (0, 1, or 2). A small amount of sialylated tetraantennary oligosaccharide was detected. Exoglycosidase digestion suggested that fucose residues were linked to reducing end GlcNAc in biantennary oligosaccharides and to reducing end and/or α1–3 to outer arms GlcNAc in triantennary oligosaccharides and that roughly one of the antennas in triantennary oligosaccharides was α2–3 sialylated and occasionally α1–3 fucosylated at GlcNAc.
© 2005 Elsevier Inc. All rights reserved.

*Keywords:* Ceruloplasmin; Glycopeptide; Liquid chromatography-electrospray tandem mass spectrometry; Product ion spectrum; Exoglycosidase digestion

Ceruloplasmin (CP)[1] is a blue copper serum glycoprotein synthesized in the liver. CP has ferroxidase activity and plays an essential role in iron metabolism [1–4]. The primary structure of human CP has been determined by amino acid sequencing, and it is composed of a single polypeptide chain of 1046 amino acid residues [5]. The amino acid sequence was confirmed from complete cDNA sequence [6]. The major oligosaccharides in human CP were reported to be sialylated bi- and triantennary structures with or without a fucose residue [7,8]. Although four N-glycosylation sites (Asn119, Asn339, Asn378, and Asn743) were identified among seven potential sites [9], the heterogeneity of oligosaccharides was still unknown at each glycosylation site. CP is an acute phase reactant, and the serum concentration increases during inflammation, infection, and trauma [10]. It is known that the patterns of glycosylation are changed by inflammatory cytokines [11]. Several studies have reported that CP is a good diagnostic marker of solid malignant tumors [12,13] and that the CP glycoform might

* Corresponding author. Fax: +81 3 3700 9084.
*E-mail address:* harazono@nihs.go.jp (A. Harazono).

[1] *Abbreviations used:* CP, ceruloplasmin; LC-ESI-MS, liquid chromatography with electrospray ionization mass spectrometry; Hex, hexose; HexNAc, *N*-acetylhexosamine; LC-ESI-MS/MS, liquid chromatography with electrospray ionization tandem mass spectrometry; EDTA, ethylenediaminetetraacetic acid; TFA, trifluoroacetic acid; Q-TOF, quadrupole time-of-flight; TIC, total ion chromatogram; NeuAc, *N*-acetylneuraminic acid; GlcNAc, *N*-acetylglucosamine; Fuc, fucose.

0003-2697/$ - see front matter © 2005 Elsevier Inc. All rights reserved.
doi:10.1016/j.ab.2005.10.036

be a valuable supplement [12]. Thus, it is important to conduct a site-specific glycosylation analysis of normal human CP.

One of the most effective techniques for determining the site-specific carbohydrate heterogeneity of glycoproteins is the mass spectrometric peptide mapping of proteolytic fragments of glycoproteins by liquid chromatography with electrospray ionization mass spectrometry (LC-ESI-MS) [14–19]. The specific detection of glycopeptides in a complex peptide mixture is generally achieved by monitoring specific carbohydrate fragment ions such as *m/z* 204 (HexNAc) and *m/z* 366 (HexHexNAc) produced by cone voltage fragmentation or by precursor ion scanning [15–19]. Because product ion spectra of glycopeptides show high abundant carbohydrate fragment ions and low abundant b- and y-series fragment ions derived from the peptide backbone [20,21], product ion spectra acquired data-dependently in liquid chromatography with electrospray ionization tandem mass spectrometry (LC-ESI-MS/MS) can be used for both the selection from the peptides and the identification of the glycopeptides [22]. MS in combination with specific exoglycosidase digestions allows us to obtain the site-specific information on anomericity and linkage of glycans [23]. In the current study, we conducted a site-specific glycosylation analysis of human CP and successfully determined glycosylation status and glycosylation profile at each N-glycosylation site.

## Materials and methods

### *Materials*

Acetonitrile, formic acid, and guanidine hydrochloride were purchased from Wako Pure Chemicals Industries (Osaka, Japan). Purified human CP was purchased from Calbiochem (San Diego, CA, USA). Modified trypsin was purchased from Promega (Madison, WI, USA). α2–3 Neuraminidase (EC 3.2.1.18) of *Macrobdella decora*, a recombinant form, and α1–3,4 fucosidase (EC 3.2.1.51) from *Xanthomonas* sp. were purchased from Calbiochem. α2–3,6,8,9 Neuraminidase (EC 3.2.1.18) of *Arthrobacter ureafaciens*, a recombinant form, and β1–4 galactosidase (EC 3.2.1.23) were purchased from Sigma Chemical (St. Louis, MO, USA). The water used was obtained from a Milli-Q water system (Millipore, Bedford, MA, USA). All other reagents were of the highest quality available.

### *Reduction and S-carboxymethylation of CP*

CP (100 μg) was dissolved in 270 μl of 0.5 M Tris–HCl buffer (pH 8.5) that contained 8 M guanidine hydrochloride and 5 mM ethylenediaminetetraacetic acid (EDTA). After the addition of 2 μl of 2-mercaptoethanol, the mixture was incubated for 2 h at 40 °C. Then 5.67 mg of monoiodoacetic acid was added, and the resulting mixture was incubated for 2 h at 40 °C in the dark. The reaction mixture was applied to a PD-10 column (Amersham Biosciences, Uppsala, Sweden) to remove the reagents, and the eluate was lyophilized.

### *Trypsin digestion of CP*

Reduced and carboxymethylated CP was redissolved in 100 μl of 0.1 M Tris–HCl buffer (pH 8.0). An aliquot of 1 μl of trypsin prepared as 1 μg/μl was added to 50 μl of CP solution (1:50, w/w), and the mixture was incubated for 16 h at 37 °C. The enzyme digestion was stopped by storing at −20 °C before analysis.

### *HPLC of tryptic digest of CP*

Tryptic digests (0.2 and 0.4 μg) of human CP were analyzed by LC-ESI-MS/MS to identify the peptides and glycopeptides, respectively. HPLC was performed on a Paradigm MS 4 (Michrome BioResources, Auburn, CA, USA) equipped with a Magic C18 column (0.2 μ, 50 mm, Michrome BioResources). The eluents consisted of water containing 2% (v/v) acetonitrile and 0.1% (v/v) formic acid (pump A) and 90% acetonitrile and 0.1% formic acid (pump B). Trypsin-digested samples were loaded onto a microtrap (peptide captrap, Michrom BioResources). After a wash with 15 μl $H_2O/CH_3CN$ (98:2) with 0.1% trifluoroacetic acid (TFA), the trapping column was switched into line with the column. Samples were eluted with 5% of B for 10 min, followed by a linear gradient from 5 to 65% of B in 60 min at a flow rate of 2 μl/min.

### *ESI-Q-TOF-MS/MS*

Mass spectrometric analyses were performed using a quadrupole time-of-flight (Q-TOF) mass spectrometer (QSTAR Pulsar, MDS Sciex, Toronto, Canada) equipped with a nano-electrospray ion source. The mass spectrometer was operated in the positive ion mode. The nanospray voltage was set at 2500 V. Mass spectra were acquired at *m/z* 400–2000 or *m/z* 1000–2000 for MS analysis and at *m/z* 100–2000 for MS/MS analysis. After every regular MS acquisition, two MS/MS acquisitions against top two of the multiply charged molecular ions were performed (data-dependent acquisition). The precursor ions with the same *m/z* as acquired previously were excluded for 120 s. The collision energy was varied between 30 and 80 eV depending on the size and charge of the molecular ion. Accumulation times for the spectra were 1.0 and 2.0 s for MS and MS/MS, respectively. All peaks were resolved monoisotopically.

Tandem MS/MS data from LC-ESI-MS/MS runs were submitted to the search engine Mascot to identify the tryptic peptides of CP. One missed cleavage was allowed, and tolerances of 2.0 and 0.8 u mass were used for precursor and product ions, respectively. From the data for LC-ESI-MS/MS at *m/z* 1000–2000, glycopeptide precursor ions were selected manually based on the presence of oligosaccharide oxonium ions such as *m/z* 204 (HexNAc) and *m/z* 366 (HexHexNAc). The glycopeptide ions were assigned based on

the presence of b- and y-series fragment ions of peptides of putative glycopeptides or molecular weight difference of sugar unit. The molecular weight of the carbohydrate in the glycopeptide was calculated from the molecular weights of the glycopeptide and the suggested peptide. The oligosaccharide composition and type were deduced from the molecular weight of the carbohydrate.

### *Oligosaccharide sequencing by exoglycosidase digestions*

Trypsin in the digest of human CP was inactivated by boiling for 5 min at 100 °C. Aliquots of the digest (4 μg) were digested in a volume of 20 μl for 12 h at 37 °C in 50 mM sodium phosphate buffer (pH 5.0) using the following exoglycosidases alone or in combination: α2–3 neuraminidase, 20 mU/ml; α2–3,6,8,9 neuraminidase, 100 mU/ml; α1–3,4 fucosidase, 20 mU/ml; and β1–4 galactosidase, 30 mU/ml. Aliquots (0.08 μg) before and after exoglycosidase digestions were subjected to LC-ESI-MS at *m/z* 700 to 2000 in which MS/MS acquisition was not performed.

## Results

### *Peptide mapping of tryptic digest of human CP (LC-ESI-MS/MS in m/z range of 400–2000)*

The amino acid sequence of human CP (National Center for Biotechnology Information protein database: P00450) is shown in Fig. 1. The tryptic peptides, including potential N-glycosylation sites, are shown in bold type. Trypsin can digest human CP into seven glycopeptides containing only one potential N-glycosylation site. To determine the glycosylation state at each glycosylation site, we performed mass spectrometric peptide mapping of the tryptic digest of CP. An aliquot of 0.2 μg of the tryptic digest was analyzed by

```
KEKHYYIGII ETTWDYASDH GEKKLISVDT EHSNIYLQNG PDRIGRLYKK ALYLQYTDET
                                                               119
FRTTIEKPVW LGFLGPIIKA ETGDKVYVHL KNLASRPYTF HSHGITYYKE HEGAIYPDNT
TDFQRADDKV YPGEQYTYML LATEEQSPGE GDGNCVTRIY HSHIDAPKDI ASGLIGPLII
                              208
CKKDSLDKEK EKHIDREFVV MFSVVDENFS WYLEDNIKTY CSEPEKVDKD NEDFQESNRM
YSVNGYTFGS LPGLSMCAED RVKWYLFGMG NEVDVHAAFF HGQALTNKNY RIDTINLFPA
                                              339
TLFDAYMVAQ NPGEWMLSCQ NLNHLKAGLQ AFFQVQECNK SSSKDNIRGK HVRHYYIAAE
                   378
EIIWNYAPSG IDIFTKENLT APGSDSAVFF EQGTTRIGGS YKKLVYREYT DASFTNRKER
GPEEEHLGIL GPVIWAEVGD TIRVTFHNKG AYPLSIEPIG VRFNKNNEGT YYSPNYNPQS
RSVPPSASHV APTETFTYEW TVPKEVGPTN ADPVCLAKMY YSAVDPTKDI FTGLIGPMKI
                              569
CKKGSLHANG RQKDVDKEFY LFPTVFDENE SLLLEDNIRM FTTAPDQVDK EDEDFQESNK
MHSMNGFMYG NQPGLTMCKG DSVVWYLFSA GNEADVHGIY FSGNTYLWRG ERRDTANLFP
QTSLTLHMWP DTEGTFNVEC LTTDHYTGGM KQKYTVNQCR RQSEDSTFYL GERTYYIAAV
                        743
EVEWDYSPQR EWEKELHHLQ EQNVSNAFLD KGEFYIGSKY KKVVYRQYTD STFRVPVERK
AEEEHLGILG PQLHADVGDK VKIIFKNMAT RPYSIHAHGV QTESSTVTPT LPGETLTYVW
KIPERSGAGT EDSACIPWAY YSTVDQVKDL YSGLIGPLIV CRRPYLKVFN PRRKLEFALL
                 907
FLVFDENESW YLDDNIKTYS DHPEKVNKDD EEFIESNKMH AINGRMFGNL QGLTMHVGDE
VNWYLMGMGN EIDLHTVHFH GHSFQYKHRG VYSSDVFDIF PGTYQTLEMF PRTPGIWLLH
CHVTDHIHAG METTYTVLQN EDTKSG
```

Fig. 1. Primary amino acid sequence of human CP (P00450). The tryptic peptides, including potential N-glycosylation sites, are shown in bold type. Tryptic peptides identified in the LC-ESI-MS/MS analysis are underlined. Cysteine residues are carboxymethylated. Identified N-glycosylation sites are indicated by arrow.

LC-ESI-MS/MS in the *m/z* range of 400–2000 (data not shown). When molecular ions with more than a single charge were detected, the product ion spectrum was acquired automatically. Peptide identification of each product ion spectrum was done using the Mascot search engine. More than 70% of the amino acid sequence was identified; identified amino acids of CP are underlined in Fig. 1. Three peptides containing the potential N-glycosylation site (Asn208, Asn569, and Asn907 [residues 197–218, 558–579, and 895–917, respectively]) were detected, whereas peptides containing the other N-glycosylation sites were not detected. Thus, Asn119, Asn339, Asn378, and Asn743 might be glycosylated.

### *Glycosylation analysis of human CP (LC-ESI-MS/MS in the m/z range of 1000–2000)*

N-glycosylated peptides have relatively high molecular weights due to their oligosaccharide moiety. Because ions at lower *m/z* values can be detected in the *m/z* range of 400–2000, glycopeptide ions with higher *m/z* values might be missed to obtain product ion spectra. To detect glycopeptide ions preferentially, another LC-ESI-MS/MS analysis was carried out in the *m/z* range of 1000–2000 using an aliquot of 0.4 μg of the tryptic digest. Fig. 2A shows a total ion chromatogram (TIC) of a TOF-MS scan for the full scan *m/z* 1000–2000. Fig. 2B shows a TIC of the product ion scan. Because product ion spectra of glycopeptide precursor ions have abundant carbohydrate B-ions, *m/z* 204 (HexNAc), *m/z* 186 (HexNAc-$H_2O$), *m/z* 366 (HexHexNAc), and *m/z* 292 (NeuAc), the extracted ion chromatogram at *m/z* 204.05–204.15 (HexNAc, 204.08) of the product ion scan is illustrated in Fig. 2C. The extracted ion chromatogram at *m/z* 204.05–204.15 of product ion spectra provides a useful indication of the selection of glycopeptide precursor ions. The glycopeptide ions were assigned based on an examination of product ion spectra using the information on amino acid sequences of the peptides containing a putative N-glycosylation site.

### *Identification of Asn119 glycopeptide*

The product ion spectrum of 1366.6 (+3) at 26 min, labeled by A in Fig. 2C, is shown in Fig. 3A. There were abundant oligosaccharide oxonium ions such as *m/z* 204 (HexNAc), *m/z* 366 (HexHexNAc), *m/z* 186 (HexNAc-$H_2O$), *m/z* 168 (HexNAc-$2H_2O$), *m/z* 274 (NeuAc-$H_2O$), and *m/z* 292 (NeuAc). Thus, this precursor ion was assigned as a glycopeptide. Several fragment ions consistent with b- and y-series fragment ions [24] derived from the peptide EHEGAIYPDN[119]TTDFQR (residues 110–125) were detected together with several deamidated (−17) or dehydrogenated (−18) b- and y-series ions and y-series ions with the GlcNAc residue. Thus, the peptide moiety EHEGA IYPDNTTDFQR was suggested. The carbohydrate's molecular weight, 2223.0, was calculated by subtracting the theoretical molecular weight of the peptide (1891.8) from

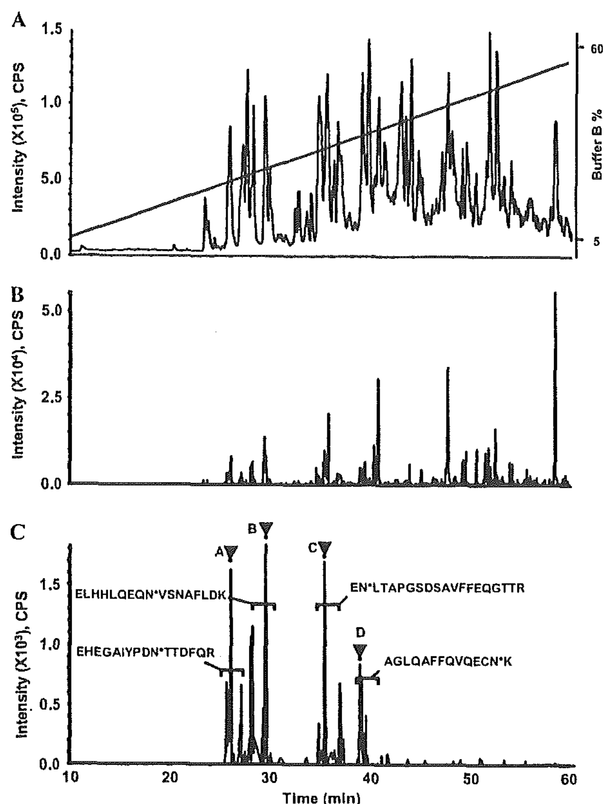


Fig. 2. LC-ESI-MS/MS in the *m/z* range of 1000–2000 of the tryptic digest of human CP. (A) TIC of the TOF-MS scan for the full-scan *m/z* 1000–2000 and the HPLC gradient. (B) TIC of the product ion scan acquired data-dependently. (C) Extracted ion chromatograph at *m/z* 204.05–204.15 of the product ion spectra. Brackets denote glycopeptide fraction and peptide sequences of the glycopeptides. Product ion spectra indicated by A–D are shown in Fig. 3.

the calculated molecular weight of the glycopeptide (4096.7) and adding the molecular weight of $H_2O$ (18.0). The presence of product ions at *m/z* 274 (NeuAc-$H_2O$) and *m/z* 292 (NeuAc) suggested sialylation of the oligosaccharide. Thus, the carbohydrate's composition, $[HexNAc]_4[Hex]_5[NeuAc]_2$, was deduced.

### *Identification of Asn743 glycopeptide*

The product ion spectrum of 1628.4 (+3) at 29 min, labeled by B in Fig. 2C, is shown in Fig. 3B. This precursor ion was assigned as a glycopeptide due to the presence of abundant oligosaccharide oxonium ions such as *m/z* 204 (HexNAc), *m/z* 366 (HexHexNAc), and *m/z* 292 (NeuAc) in the product ion spectrum. Several fragment ions were consistent with theoretical b- and y-series fragment ions derived from the peptide ELHHLQEQN$^{743}$VSNAFLDK (residues 735–751). Doubly charged ions of peptide (*m/z* 1011.7), peptide + HexNAc (*m/z* 1113.1), peptide + 2HexNAc (*m/z* 1214.6), peptide + 2HexNAc + Hex (*m/z* 1295.5), peptide + 2HexNAc + 2Hex (*m/z* 1376.7), and peptide + 2HexNAc + 3Hex (*m/z* 1457.5) showed the sequential fragmentation of the pentasaccharide carbohydrate core. The carbohydrate's molecular weight, 2879.1, was calculated from the theoretical molecular weight of the peptide (2021.0) and the calculated molecular weight of the glycopeptide (4882.1). The carbohydrate's composition, $[HexNAc]_5[Hex]_6[NeuAc]_3$, was deduced from the molecular weight.

### *Identification of Asn378 glycopeptide*

The product ion spectrum of 1444.6 (+3) at 35 min, labeled by C in Fig. 2C, is shown in Fig. 3C. Abundant oligosaccharide oxonium ions were detected, as were several fragment ions consistent with b- and y-series fragment ions derived from the peptide EN$^{378}$LTAPGSDSAVFFEQGTTR (residues 377–391). The carbohydrate's molecular weight, 2222.9, was calculated from the theoretical molecular weight of the peptide (2126.0) and the calculated molecular weight of the glycopeptide (4330.9). Thus, the peptide moiety ENLTAPGSDSAVFFEQGTTR and the carbohydrate's composition, $[HexNAc]_4[Hex]_5[NeuAc]_2$, were suggested.

### *Identification of Asn339 glycopeptide*

The product ion spectrum of 1282.6 (+3) at 39 min, labeled by D in Fig. 2C, is shown in Fig. 3C. The spectrum contains abundant oligosaccharide oxonium ions, and several fragment ions consistent with b- and y-series fragment ions derived from the peptide AGLQAFFQVQECN$^{339}$K (residues 327–340) were detected. The product ion spectrum contains the ions of the peptide (*m/z* 1640.8) and peptide + HexNAc (*m/z* 1843.9) and several y-series fragment ions of the peptide with a GlcNAc residue. The carbohydrate's molecular weight, 2223.0, was calculated from the theoretical molecular weight of the peptide (1639.7) and the calculated molecular weight of the glycopeptide (3844.7). Thus, the peptide moiety AGLQAFFQVQECNK and the carbohydrate's composition, $[HexNAc]_4[Hex]_5[NeuAc]_2$, were suggested.

### *Heterogeneity of oligosaccharides at each glycosylation site*

Glycopeptides with the potential N-glycosylation sites Asn119, Asn339, Asn378, and Asn743 were detected, whereas no glycopeptides containing the other sites (Asn208, Asn569, and Asn907) could be detected in this LC-ESI-MS/MS analysis. These findings suggest that Asn119, Asn339, Asn378, and Asn743 of human CP are glycosylated and that Asn208, Asn569, and Asn907 are not. Once a glycopeptide was identified, the other glycopeptides with the same peptide could be easily assigned because they were eluted at a similar retention time in the order of the number of NeuAc and had similar product ion spectra and molecular weight difference of sugar units. The oligosaccharide heterogeneity at each four N-glycosylation sites was determined by mass spectrum. For a representative example, the mass spectrum of the glycopeptides containing

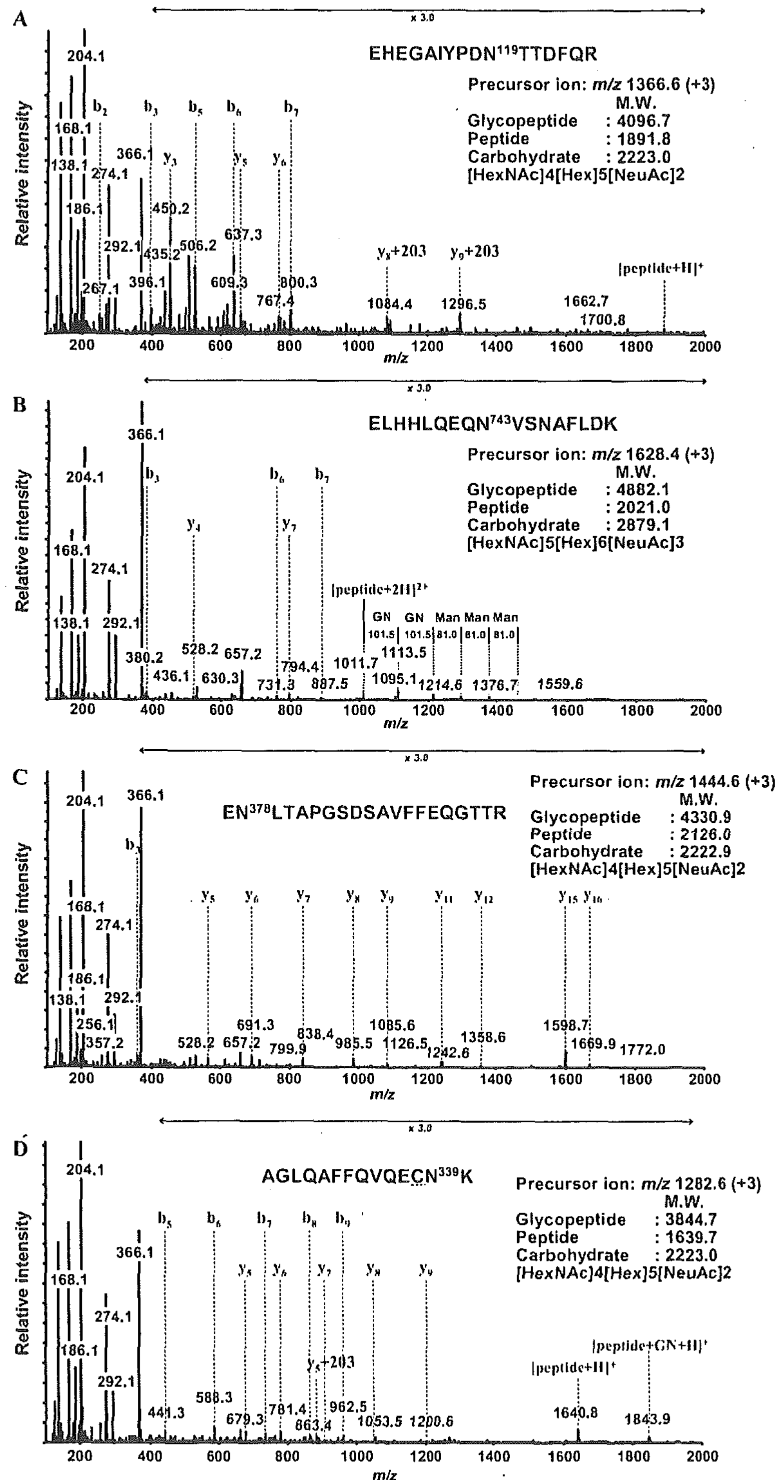


Fig. 3. Product ion spectra of *m/z* 1366.6 (+3) at 26 min (A), *m/z* 1628.4 (+3) at 29 min (B), *m/z* 1444.6 (+3) at 35 min (C), and *m/z* 1282.6 (+3) at 39 min (D) labeled by A, B, C, and D, respectively, in Fig. 2C. These spectra show abundant carbohydrate-derived ions at *m/z* 168 (HexNAc-2$H_2O$), *m/z* 186 (HexNAc-$H_2O$), *m/z* 204 (HexNAc), *m/z* 366 (HexHexNAc), *m/z* 274 (NeuAc-$H_2O$), and *m/z* 292 (NeuAc). The b- and y-series fragment ions [24] derived from the peptide moiety were observed. The molecular weights of the oligosaccharide were calculated from the molecular weights of the glycopeptide and peptide, and the deduced oligosaccharide composition is presented. Cystein residue was carboxymethylated.

Asn743 at 27.5 to 31.5 min is shown Fig. 4. The results of glycosylation analysis are summarized in Table 1. Deduced compositions of the oligosaccharides are estimated based on the calculated molecular weights of the oligosaccharides. Relative peak intensity was calculated by comparing triply charged glycopeptide ions. All glycosylation sites were occupied by at least three kinds of oligosaccharides, namely disialobiantennary structures ($[HexNAc]_4[Hex]_5[NeuAc]_2$), disialobiantennary structures with fucose ($[HexNAc]_4[Hex]_5[NeuAc]_2[Fuc]_1$), and trisialotriantennary structures ($[HexNAc]_5[Hex]_6[NeuAc]_3$). Trisialotriantennary structures with one fucose or two fucoses ($[HexNAc]_5[Hex]_6[NeuAc]_3[Fuc]_{1-2}$) were also detected at Asn119 and Asn743; furthermore, tetrasialotetraantennary structures with no fucose or one fucose ($[HexNAc]_6[Hex]_7[NeuAc]_4[Fuc]_{0-1}$) were detected at Asn743.

*Linkage analysis of oligosaccharides by exoglycosydase digestion*

To elucidate the oligosaccharide structure in terms of sequence and linkage, aliquots of the tryptic digest were further digested with exoglycosidases. As a representative example, Fig. 5 shows integrated mass spectra during the periods at which Asn119 glycopeptides were eluted in LC-ESI-MS analyses before and after digestion with exoglycosidase arrays. Treatment with α2–3 neuraminidase removed one NeuAc residue from most of the triantennary structures ($[HexNAc]_5[Hex]_6[NeuAc]_3[Fuc]_{0-2}$) and a small amount of biantennary structures ($[HexNAc]_4[Hex]_5[NeuAc]_2[Fuc]_{0-1}$) (Fig. 5B). A minor amount of triantennary structures removed two NeuAc residues. Thus, it appears that most triantennary structures contain one α2–3-linked NeuAc. Treatment with α2–3 neuraminidase + β1–4 galactosidase removed all terminal galactose residues from the desialylated glycans without fucose residues but only partially digested terminal galactoses from the desialylated glycans with fucoses (Fig. 5C). The addition of α1–3,4 fucosidase to α2–3 neuraminidase + β1–4 galactosidase treatment completely digested the remaining terminal galactose by releasing one fucose and one galactose (Fig. 5D). Thus, galactose residues are linked β1–4 to GlcNAc, and undigestion of terminal galactose by β1–4 galactosidase is due to attachment of fucose [25,26]. Because galactose was linked to GlcNAc in the β1–4 position, the fucose removed with α1–3,4 fucosidase may be linked α1–3 to GlcNAc but not α1–4 to GlcNAc. These data strongly suggested that sialyl Lewis X structure was present in human CP. Sialyl Lewis X structure was present predominantly in triantennary oligosaccharides, but a small amount seemed to be present in biantennary oligosaccharides as well. The remaining fucose residue may be linked α1–6 to reducing end GlcNAc (core fucose).

Fig. 6 shows integrated mass spectra of Asn119, Asn743, Asn378, and Asn339 glycopeptides in LC-ESI-MS analysis following digestion with α2–3,6,8,9 neuraminidase + β1–4 galactosidase. Treatment with α2–3,6,8,9 neuraminidase + β1–4 galactosidase removed all NeuAc and then removed terminal galactoses in the outer arms without fucose. Thus, this treatment could differentiate glycoforms based on the location of fucose residues. Fucosylation occurred predominantly at reducing end GlcNAc in biantennary oligosaccharides and occurred at reducing end GlcNAc and/or outer arm GlcNAc in triantennary oligosaccharides. Mass spectra of Asn119 and Asn743 glycopeptides showed higher oligosaccharide heterogeneity, and a minor amount of tetraantennary glycans could be detected. The glycosylation profile

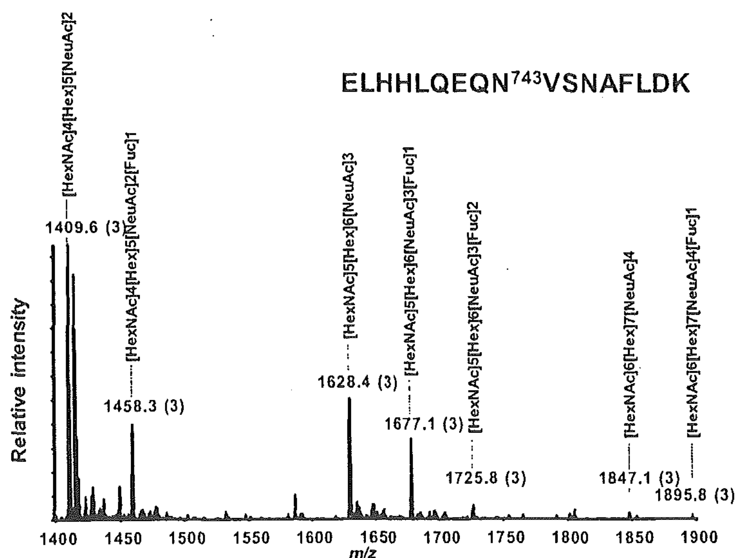


Fig. 4. Mass spectrum of the glycopeptides containing Asn743 eluting at 27.5–31.5 min from Fig. 2A. Deduced composition of the oligosaccharides is indicated based on the molecular weights of the oligosaccharides.

Table 1
Results of site-specific glycosylation analysis of human CP

| Retention time (min) | Glycopeptides | | Calculated MW | Relative peak intensity[a] (%) | Peptide | | Oligosaccharide | | |
|---|---|---|---|---|---|---|---|---|---|
| | *m/z* | Charge | | | Sequence | Theoretical MW | Calculated MW | Theoretical MW | Composition[b,c] |
| 26 | 1415.3 | +3 | 4242.8 | 52 | EHEGAIYPDN$^{119}$TTDFQR | 1891.8 | 2369.0 | 2368.8 | [HexNAc]4[Hex]5[NeuAc]2[Fuc]1 |
| 26 | 1366.6 | +3 | 4096.7 | 100 | EHEGAIYPDN$^{119}$TTDFQR | 1891.8 | 2223.0 | 2222.8 | [HexNAc]4[Hex]5[NeuAc]2 |
| 27 | 1682.7 | +3 | 5045.1 | 6 | EHEGAIYPDN$^{119}$TTDFQR | 1891.8 | 3171.3 | 3171.1 | [HexNAc]5[Hex]6[NeuAc]3[Fuc]2 |
| 27 | 1634.0 | +3 | 4899.0 | 21 | EHEGAIYPDN$^{119}$TTDFQR | 1891.8 | 3025.2 | 3025.1 | [HexNAc]5[Hex]6[NeuAc]3[Fuc]1 |
| 27 | 1225.8 | +4 | 4899.0 | | | | | | |
| 27 | 1585.3 | +3 | 4753.0 | 24 | EHEGAIYPDN$^{119}$TTDFQR | 1891.8 | 2879.2 | 2879.0 | [HexNAc]5[Hex]6[NeuAc]3 |
| 27 | 1189.3 | +4 | 4753.0 | | | | | | |
| 28 | 1458.3 | +3 | 4372.0 | 35 | ELHHLQEQN$^{743}$VSNAFLDK | 2021.0 | 2369.0 | 2368.8 | [HexNAc]4[Hex]5[NeuAc]2[Fuc]1 |
| 28 | 1409.6 | +3 | 4225.9 | 100 | ELHHLQEQN$^{743}$VSNAFLDK | 2021.0 | 2222.9 | 2222.8 | [HexNAc]4[Hex]5[NeuAc]2 |
| 28 | 1057.5 | +4 | 4225.9 | | | | | | |
| 29 | 1725.8 | +3 | 5174.5 | 5 | ELHHLQEQN$^{743}$VSNAFLDK | 2021.0 | 3171.5 | 3171.1 | [HexNAc]5[Hex]6[NeuAc]3[Fuc]2 |
| 29 | 1294.6 | +4 | 5174.2 | | | | | | |
| 29 | 1677.1 | +3 | 5028.2 | 29 | ELHHLQEQN$^{743}$VSNAFLDK | 2021.0 | 3025.3 | 3025.1 | [HexNAc]5[Hex]6[NeuAc]3[Fuc]1 |
| 29 | 1258.1 | +4 | 5028.2 | | | | | | |
| 29 | 1628.4 | +3 | 4882.1 | 43 | ELHHLQEQN$^{743}$VSNAFLDK | 2021.0 | 2879.1 | 2879.0 | [HexNAc]5[Hex]6[NeuAc]3 |
| 29 | 1221.5 | +4 | 4882.1 | | | | | | |
| 31[d] | 1895.8 | +3 | 5684.4 | 2 | ELHHLQEQN$^{743}$VSNAFLDK | 2021.0 | 3681.4 | 3681.3 | [HexNAc]6[Hex]7[NeuAc]4[Fuc]1 |
| 31[d] | 1422.1 | +4 | 5684.3 | | | | | | |
| 31[d] | 1847.1 | +3 | 5538.4 | 3 | ELHHLQEQN$^{743}$VSNAFLDK | 2021.0 | 3535.4 | 3535.2 | [HexNAc]6[Hex]7[NeuAc]4 |
| 31 | 1385.6 | +4 | 5538.3 | | | | | | |
| 35[d] | 1493.3 | +3 | 4477.0 | 6 | EN$^{378}$LTAPGSDSAVFFEQGTTR | 2126.0 | 2369.0 | 2368.8 | [HexNAc]4[Hex]5[NeuAc]2[Fuc]1 |
| 35 | 1444.6 | +3 | 4330.9 | 100 | EN$^{378}$LTAPGSDSAVFFEQGTTR | 2126.0 | 2222.9 | 2222.8 | [HexNAc]4[Hex]5[NeuAc]2 |
| 37 | 1712.1 | +3 | 5133.2 | 8 | EN$^{378}$LTAPGSDSAVFFEQGTTR | 2126.0 | 3025.2 | 3025.1 | [HexNAc]5[Hex]6[NeuAc]3[Fuc]1 |
| 37 | 1284.3 | +4 | 5133.2 | | | | | | |
| 37 | 1663.4 | +3 | 4987.1 | 23 | EN$^{378}$LTAPGSDSAVFFEQGTTR | 2126.0 | 2879.2 | 2879.0 | [HexNAc]5[Hex]6[NeuAc]3 |
| 37 | 1247.8 | +4 | 4987.2 | | | | | | |
| 39 | 1331.3 | +3 | 3990.8 | 14 | AGLQAFFQVQECN$^{339}$K | 1639.7 | 2369.1 | 2368.8 | [HexNAc]4[Hex]5[NeuAc]2[Fuc]1 |
| 39 | 1923.4 | +2 | 3844.7 | | AGLQAFFQVQECN$^{339}$K | 1639.7 | 2223.0 | 2222.8 | [HexNAc]4[Hex]5[NeuAc]2 |
| 39 | 1282.6 | +3 | 3844.7 | 100 | | | | | |
| 41 | 1501.3 | +3 | 4500.8 | 6 | AGLQAFFQVQECN$^{339}$K | 1639.7 | 2879.2 | 2879.0 | [HexNAc]5[Hex]6[NeuAc]3 |

*Note.* All masses are monoisotopic. Cysteine residue was carboxymethylated.

[a] Relative peak intensity was calculated by comparing same charge state glycopeptide ions. The intensity of the glycoform with maximum at each glycosylation site was taken as 100%.

[b] The oligosaccharide composition was deduced from the molecular weight of the oligosaccharide.

[c] The glycopeptide ions adducted by $NH_4^+$ or $Na^+$ were excluded.

[d] Product ion spectra of these molecular ions were not acquired. However, these were considered glycopeptides because of a molecular weight difference of 146 (Fuc) and the same retention time as other glycopeptides.

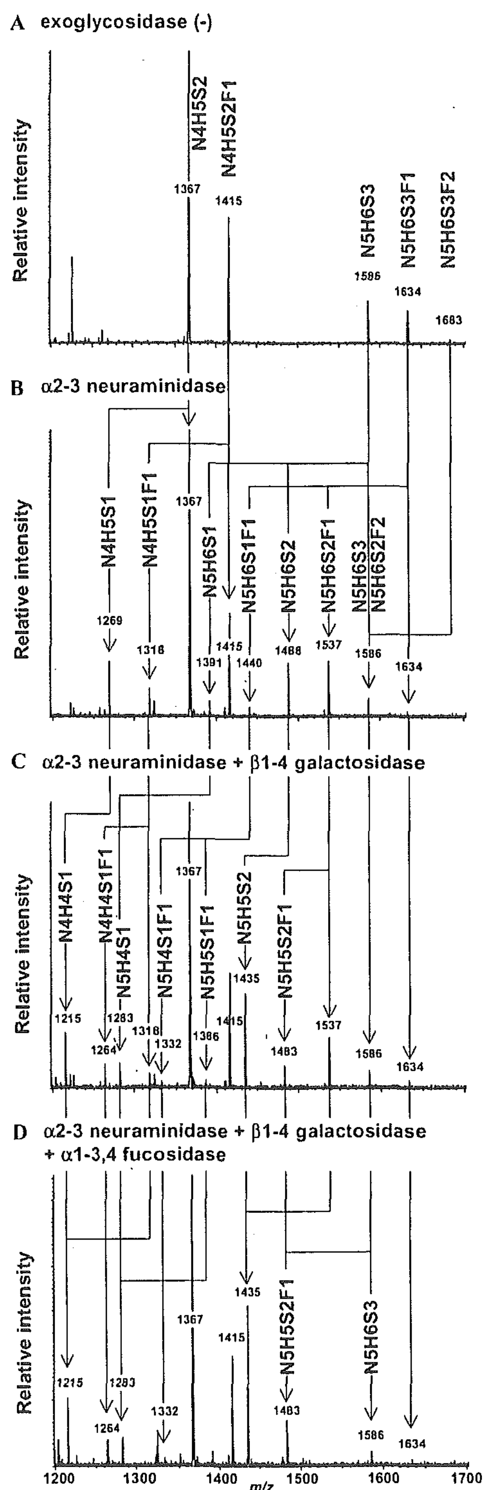


Fig. 5. LC-ESI mass spectra of the glycopeptides containing Asn119 digested with the following exoglycosidases: (A) exoglycosidase (−); (B) α2–3 neuraminidase; (C) α2–3 neuraminidase + β1–4 galactosidase; (D) α2–3 neuraminidase + β1–4 galactosidase + α1–3,4 fucosidase. Arrows between panels A and B, panels B and C, and panels C and D correspond to the digestion of NeuAc, Gal, and Gal+Fuc, respectively. H, hexose; N, *N*-acetylhexosamine; F, fucose; S, *N*-acetylneuraminic acid.

of Asn378 glycopeptides showed lower core fucosylation, and that of Asn339 glycopeptides showed lower branching. These glycosylation profiles provided the heterogeneity of fucose linkage and the number of arms at each glycosylationsite in human CP.

## Discussion

A site-specific glycosylation analysis of human CP was conducted using LC-ESI-MS/MS, where product ion spectra were acquired in a data-dependent manner. The collision energy for the product ion scan was adjusted from 30 to 80 eV depending on the size and charge of the precursor ion. Under these conditions, peptide precursor ions were degraded and produced b- and y-series fragment ions derived from the amino acid sequence. Glycopeptide precursor ions produced abundant carbohydrate ions (*m/z* 204, 186, 168, and 366) together with several low intensity b- and y-series fragment ions derived from the amino acid sequence [20,21]. Thus, product ion spectra of glycopeptides are readily distinguishable from those of peptides by such carbohydrate marker ions, and the peptide moiety in the glycopeptide could be deduced from the product ions that were consistent with the expected fragment ions derived from the peptide containing the N-glycosylation site. It is known that the glycopeptide ions are more labile than peptide ions and produce consecutive monosaccharide/polysaccharide losses at much lower collision energy, and this would provide information about branching and fucose location [18]. However, we used relatively high collision energy in this site-specific glycosylation analysis to identify the peptide ions in parallel with the detection and identification of the glycopeptide ions.

Protein coverage of more than 70% in human CP was obtained in the LC-ESI-MS/MS analysis with the *m/z* range of 400–2000 (for peptide mapping). The heterogeneity at four potential N-glycosylation sites was determined in the *m/z* range of 1000–2000 (glycosylation analysis). We could detect all of the potential glycosylation sites as either glycopeptides or nonglycosylated peptides. Peptides containing the potential N-glycosylation site Asn208, Asn569, or Asn907 were detected in nonglycosylated but not glycosylated forms. Peptides with the potential N-glycosylation site Asn119, Asn339, Asn378 or Asn743 were detected in glycosylated but not nonglycosylated forms. These findings indicate that Asn119, Asn339, Asn378, and Asn743 of human CP are glycosylated and that Asn208, Asn569, and Asn907 are not. Human CP was reported to have no O-linked glycosylation [8]. No information on O-glycosylation was obtained from this analysis. These results are consistent with a previous study determining the glycosylation sites of human CP [9].

Heterogeneity of oligosaccharides was determined at each of four glycosylation sites. Disialobiantennary structures with no fucose or one fucose ($[HexNAc]_4$ $[Hex]_5$ $[NeuAc]_2[Fuc]_{0-1}$) and trisialotriantennary structures

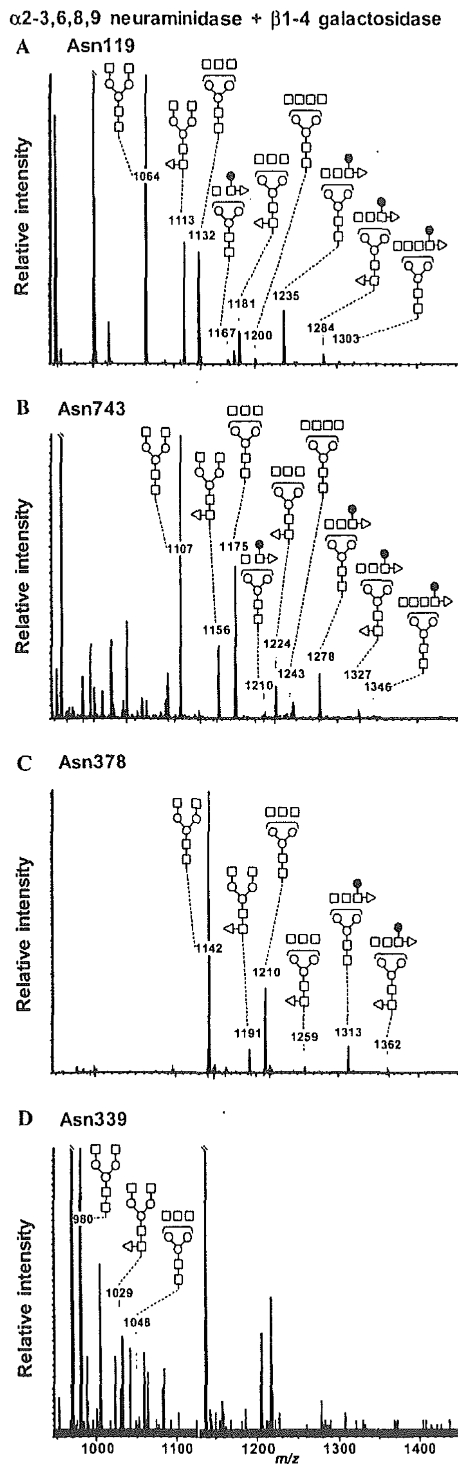


Fig. 6. LC-ESI mass spectra of the glycopeptides containing Asn119 (A), Asn743 (B), Asn378 (C), and Asn339 (D) after digestion with α2–3,6,8,9 neuraminidase + β1–4 galactosidase. Glycosylation profiles showed different degrees of branching and fucosylation at core GlcNAc and outer arm GlcNAc between glycosylation sites. Open circles, mannose; closed circles, galactose; open squares, *N*-acetyl glucosamine; open triangles, fucose.

($[HexNAc]_5[Hex]_6[NeuAc]_3$) were observed at all sites. These dominant oligosaccharides were consistent with structures published previously [7,8]. Furthermore, we detected trisialotriantennary structures with one fucose ($[HexNAc]_5[Hex]_6[NeuAc]_3[Fuc]_1$) at Asn119, Asn378, and Asn743, trisialotriantennary structures with two fucoses ($[HexNAc]_5[Hex]_6[NeuAc]_3[Fuc]_2$) at Asn119 and Asn743, and tetrasialotetraantennary structures with no fucose or one fucose ($[HexNAc]_6[Hex]_7[NeuAc]_4[Fuc]_{0-1}$) at Asn743.

To determine the linkage of fucose and NeuAc, exoglycosidase digestions were performed. Treatment with α2–3 neuraminidase suggested that roughly one antenna of triantennary glycans was linked by NeuAc in the α2–3 position. This is consistent with the previous findings that NeuAc is linked α2–3 to the Galβ1–4GlcNAcβ1–4Manα1–3Manβ1–4GlcNAcβ1–4GlcNAc group in the triantennary glycan in human CP [7,8]. Results from α2–3 neuraminidase + β1–4 galactosidase treatments with or without α1–3,4 fucosidase suggested that fucose residues were linked to reducing end GlcNAc and/or outer arm GlcNAc in the α1–3 position in the antenna where NeuAc is linked to galactose in the α2–3 position. These findings indicated that human CP contains a certain amount of sialyl Lewis X structure in triantennary glycans. Treatment with α2–3,6,8,9 neuraminidase + β1–4 galactosidase reveals the heterogeneity of the location of fucosylation as well as the number of arms. Although relative peak intensity does not express the relative amount of each glycan due to the different ionization efficiencies, the mass spectra showed the difference in fucosylation pattern and number of arms among sites.

No asialo oligosaccharides were detected in this analysis. It is known that desialylated CP is rapidly cleared from the circulation by the asialoglycoprotein receptor within the parenchymal cells of liver [27,28]. It is possible that desialylated CP might be cleared immediately by the liver.

Although the N-linked carbohydrate structures linked to human CP have been studied, only a few carbohydrate structures have been reported and site-specific characterization of these oligosaccharides has not been described. To determine the glycosylation state at each glycosylation site, the tryptic digest was examined by LC-ESI-MS/MS, where product ion spectra were acquired data-dependently. Glycopeptide ions were assigned based on the product ion spectra. Fucose and NeuAc linkages were determined by exoglycosidase digestions. Our data successfully provided comprehensive information on the site-specific N-linked oligosaccharides in human CP. This method is a powerful technique for elucidating the glycosylation of a biological sample.

## Acknowledgments

This study was supported by a Grant-in-Aid for Research on Health Sciences focusing on Drug Innovation from the Japan Health Sciences Foundation.

## References


[1] S. Osaki, D.A. Johnson, E. Frieden, The possible significance of the ferrous oxidase activity of ceruloplasmin in normal human serum, J. Biol. Chem. 241 (1966) 2746–2751.

[2] K. Yoshida, K. Furihata, S. Takeda, A. Nakamura, K. Yamamoto, H. Morita, S. Hiyamuta, S. Ikeda, N. Shimizu, N. Yanagisawa, A mutation in the ceruloplasmin gene is associated with systemic hemosiderosis in humans, Nat. Genet. 9 (1995) 267–272.

[3] Z.L. Harris, Y. Takahashi, H. Miyajima, M. Serizawa, R.T. MacGillivray, J.D. Gitlin, Aceruloplasminemia: molecular characterization of this disorder of iron metabolism, Proc. Natl. Acad. Sci. USA 92 (1995) 2539–2543.

[4] Z.L. Harris, A.P. Durley, T.K. Man, J.D. Gitlin, Targeted gene disruption reveals an essential role for ceruloplasmin in cellular iron efflux, Proc. Natl. Acad. Sci. USA 96 (1996) 10812–10817.

[5] N. Takahashi, T.L. Ortel, F.W. Putnam, Single-chain structure of human ceruloplasmin: the complete amino acid sequence of the whole molecule, Proc. Natl. Acad. Sci. USA 81 (1984) 390–394.

[6] M.L. Koschinsky, W.D. Funk, B.A. van Oost, R.T. MacGillivray, Complete cDNA sequence of human preceruloplasmin, Proc. Natl. Acad. Sci. USA 83 (1986) 5086–5090.

[7] K. Yamashita, C.J. Liang, S. Funakoshi, A. Kobata, Structural studies of asparagine-linked sugar chains of human ceruloplasmin. Structural characteristics of the triantennary complex type sugar chains of human plasma glycoproteins, J. Biol. Chem. 256 (1981) 1283–1289.

[8] M. Endo, K. Suzuki, K. Schmid, B. Fournet, Y. Karamanos, J. Montreuil, L. Dorland, H. van Halbeek, J.F. Vliegenthart, The structures and microheterogeneity of the carbohydrate chains of human plasma ceruloplasmin: a study employing 500-MHz $^1$H-NMR spectroscopy, J. Biol. Chem. 257 (1982) 8755–8760.

[9] N. Takahashi, Y. Takahashi, T.L. Ortel, J.N. Lozier, N. Ishioka, F.W. Putnam, Purification of glycopeptides of human plasma proteins by high-performance liquid chromatography, J. Chromatogr. 317 (1984) 11–26.

[10] R.J. Cousins, Absorption, transport, and hepatic metabolism of copper and zinc: special reference to metallothionein and ceruloplasmin, Physiol. Rev. 65 (1985) 238–309.

[11] A. Mackiewicz, M.K. Ganapathi, D. Schultz, I. Kushner, Monokines regulate glycosylation of acute-phase proteins, J. Exp. Med. 166 (1987) 253–258.

[12] J.E. Hansen, J. Iversen, A. Lihme, T.C. Bog-Hansen, Acute phase reaction, heterogeneity, and microheterogeneity of serum proteins as nonspecific tumor markers in lung cancer, Cancer 60 (1987) 1630–1635.

[13] A. Senra Varela, J.J. Lopez Saez, D. Quintela Senra, Serum ceruloplasmin as a diagnostic marker of cancer, Cancer Lett. 121 (1997) 139–145.

[14] V. Ling, A.W. Guzzetta, E. Canova-Davis, J.T. Stults, W.S. Hancock, T.R. Covey, B.I. Shushan, Characterization of the tryptic map of recombinant DNA derived tissue plasminogen activator by high-performance liquid chromatography-electrospray ionization mass spectrometry, Anal. Chem. 63 (1991) 2909–2915.

[15] S.A. Carr, M.J. Huddleston, M.F. Bean, Selective identification and differentiation of N- and O-linked oligosaccharides in glycoproteins by liquid chromatography–mass spectrometry, Protein Sci. 2 (1993) 183–196.

[16] M.J. Huddleston, M.F. Bean, S.A. Carr, Collisional fragmentation of glycopeptides by electrospray ionization LC/MS and LC/MS/MS: methods for selective detection of glycopeptides in protein digests, Anal. Chem. 65 (1993) 877–884.

[17] P.A. Schindler, C.A. Settineri, X. Collet, C.J. Fielding, A.L. Burlingame, Site-specific detection and structural characterization of the glycosylation of human plasma proteins lecithin:cholesterol acyltransferase and apolipoprotein D using HPLC/electrospray mass spectrometry and sequential glycosidase digestion, Protein Sci. 4 (1995) 791–803.

[18] M.A. Ritchie, A.C. Gill, M.J. Deery, K. Lilley, Precursor ion scanning for detection and structural characterization of heterogeneous glycopeptide mixtures, J. Am. Soc. Mass Spectrom. 13 (2002) 1065–1077.

[19] F. Wang, A. Nakouzi, R.H. Angeletti, A. Casadevall, Site-specific characterization of the N-linked oligosaccharides of a murine immunoglobulin M by high-performance liquid chromatography/electrospray mass spectrometry, Anal. Biochem. 314 (2003) 266–280.

[20] J.F. Nemeth, G.P. Hochgesang Jr., L.J. Marnett, R.M. Caprioli, Characterization of the glycosylation sites in cyclooxygenase-2 using mass spectrometry, Biochemistry 40 (2001) 3109–3116.

[21] O. Krokhin, W. Ens, K.G. Standing, J. Wilkins, H. Perreault, Site-specific N-glycosylation analysis: matrix-assisted laser desorption/ionization quadrupole–quadrupole time-of-flight tandem mass spectral signatures for recognition and identification of glycopeptides, Rapid Commun. Mass Spectrom. 18 (2004) 2020–2030.

[22] A. Harazono, N. Kawasaki, T. Kawanishi, T. Hayakawa, Site-specific glycosylation analysis of human apolipoprotein B100 using LC/ESI MS/MS, Glycobiology 15 (2005) 447–462.

[23] C.W. Sutton, J.A. O'Neill, J.S. Cottrell, Site-specific characterization of glycoprotein carbohydrates by exoglycosidase digestion and laser desorption mass spectrometry, Anal. Biochem. 218 (1994) 34–46.

[24] P. Roepstorff, J. Fohlman, Proposal for a common nomenclature for sequence ions in mass spectra of peptides, Biomed. Mass Spectrom. 11 (1984) 601.

[25] K. Maemura, M. Fukuda, Poly-*N*-acetyllactosaminyl *O*-glycans attached to leukosialin: the presence of sialyl Le(x) structures in *O*-glycans, J. Biol. Chem. 267 (1992) 24379–24386.

[26] S. Hemmerich, S.D. Rosen, 6'-Sulfated sialyl Lewis X is a major capping group of GlyCAM-1, Biochemistry 33 (1994) 4830–4835.

[27] C.J. Van Den Hamer, A.G. Morell, I.H. Scheinberg, J. Hickman, G. Ashwell, Physical and chemical studies on ceruloplasmin: IX. The role of galactosyl residues in the clearance of ceruloplasmin from the circulation, J. Biol. Chem. 245 (1970) 4397–4402.

[28] A.G. Morell, G. Gregoriadis, I.H. Scheinberg, J. Hickman, G. Ashwell, The role of sialic acid in determining the survival of glycoproteins in the circulation, J. Biol. Chem. 246 (1971) 1461–1467.

ELSEVIER

Available online at www.sciencedirect.com

SCIENCE DIRECT®

Journal of Chromatography A, 1103 (2006) 296–306

JOURNAL OF CHROMATOGRAPHY A

www.elsevier.com/locate/chroma

# N-linked oligosaccharide analysis of rat brain Thy-1 by liquid chromatography with graphitized carbon column/ion trap-Fourier transform ion cyclotron resonance mass spectrometry in positive and negative ion modes

Satsuki Itoh [a], Nana Kawasaki [a,b,*], Noritaka Hashii [b], Akira Harazono [a], Yukari Matsuishi [a], Takao Hayakawa [c], Toru Kawanishi [a]

[a] *Division of Biological Chemistry and Biologicals, National Institute of Health Science, 1-18-1 Kamiyoga, Setagaya-ku, Tokyo 158-8501, Japan*
[b] *CREST, Japan Science and Technology Agency (JST), Japan*
[c] *Pharmaceutical and Medical Devices Agency, 3-3-2 Kasumigaseki, Chiyoda-ku, Tokyo 100-0013, Japan*

Received 25 July 2005; received in revised form 10 November 2005; accepted 14 November 2005
Available online 20 December 2005

**Abstract**

We have previously described the site-specific glycosylation analysis of rat brain Thy-1 by LC/multistage tandem mass spectrometry ($MS^n$) using proteinase-digested Thy-1. In the present study, detailed structures of oligosaccharides released from Thy-1 were elucidated by mass spectrometric oligosaccharide profiling using LC/MS with a graphitized carbon column (GCC–LC/MS). First, using model oligosaccharides, we improved the oligosaccharide profiling by ion trap mass spectrometry (IT–MS) coupled with Fourier transform ion cyclotron resonance mass spectrometry (FT–ICR–MS). Sequential scanning of a full $MS^1$ scan with FT–ICR–MS followed by data-dependent $MS^n$ with IT–MS in positive ion mode, and a subsequent full $MS^1$ scan with FT–ICR–MS followed by data-dependent $MS^n$ with IT–MS in negative ion mode enabled the monosaccharide composition analysis as well as profiling and sequencing of both neutral and acidic oligosaccharides in a single analysis. The improved oligosaccharide profiling was applied to elucidation of N-linked oligosaccharides from Thy-1 isolated by sodium dodecyl sulfate-polyacrylamide gel electrophoresis. It was demonstrated that Thy-1 possesses a significant variety of N-linked oligosaccharides, including Lewis a/x, Lewis b/y, and disialylated structure as a partial structure. Our method could be applicable to analysis of a small abundance of glycoproteins, and could become a powerful tool for glycoproteomics.
© 2005 Elsevier B.V. All rights reserved.

*Keywords:* Mass spectrometric oligosaccharide profiling; Graphitized carbon column; Ion trap mass spectrometry; Fourier transform ion cyclotron resonance mass spectrometry; Data-dependent $MS^n$; Thy-1

## 1. Introduction

Glycosylation is one of the most abundant post-translational modifications of proteins [1]. It is already known that glycosylation influences the biological functions as well as the physicochemical properties of proteins, i.e., folding, solubility, aggregation, and stability. A number of reports have noted a positive relationship between a change in glycosylation and development, aging, and certain diseases [2–4]. Elucidation of structural detail in oligosaccharides is necessary to clarify the biological properties of glycoproteins.

MS is now a powerful tool for structural analysis of glycoproteins. There are two major mass spectrometric approaches to the structural analysis of glycoproteins, i.e., MS of glycopeptides [5–7] and of oligosaccharides [8–13]. For oligosaccharide sequencing, tandem mass spectrometry as well as exoglycosidase digestions in conjuction with MS is recognized as an effective means of oligosaccharide sequencing [14–16]. Mass spectrometric peptide/glycopeptide mapping by LC coupled with tandem mass spectrometry (LC/MS/MS) is effective for the determination of glycosylation sites and the analysis of site-specific heterogeneity [17–22]. However, structural detail in

* Corresponding author. Division of Biological Chemistry and Biologicals, National Institute of Health Science, 1-18-1, Kamiyoga, Setagaya-ku, Tokyo 158-8501, Japan. Tel.: +81 3 3700 1141; fax: +81 3 3707 6950.
*E-mail address:* nana@nihs.go.jp (N. Kawasaki).

0021-9673/$ – see front matter © 2005 Elsevier B.V. All rights reserved.
doi:10.1016/j.chroma.2005.11.043

oligosaccharides is not always available by product ion spectra of glycopeptides, as many of the precursor ions consist of uniform peptides carrying different oligosaccharides with identical $m/z$ values. LC/MS/MS of glycopeptides has limitations for the structural analysis of carbohydrates due to the difficulty of isolating of glycopeptide isomers. Mass spectrometric oligosaccharide profiling through the separation of isomers by LC can supply the structural detail of each oligosaccharide although it cannot provide information regarding glycosylation sites and site-specific glycosylation [23–29]. MS of both glycopeptides and oligosaccharides is needed for glycosylation analysis of a glycoprotein [30].

Thy-1 is a cell adhesion molecule that belongs to the immunoglobulin superfamily and is attached to the cell membrane via a glycosylphosphatidylinositol (GPI)-anchor. We recently, studied the glycosylation of Thy-1 in rat brain by mass spectrometric peptide/glycopeptide mapping, and demonstrated that Thy-1 possesses various *N*-glycans at Asn23, 74, and 98 [31]. The monosaccharide composition of *N*-glycan at each glycosylation site was estimated by masses of molecular ions; however, structural detail regarding some of the oligosaccharides could not be elucidated by $MS^n$ since many glycopeptides with identical $m/z$ values contained several oligosaccharide isomers and yielded product ions from a mixture of these glycopeptide isomers. Mass spectrometric oligosaccharide profiling is necessary for detailed structural analysis of oligosaccharides.

We have previously demonstrated a simple means of oligosaccharide profiling using liquid chromatography/electrospray ionization mass spectrometry with a graphitized carbon column (GCC–LC/MS) [32–34], in which oligosaccharides can be separated on the basis of their branching, sequence, and linkage, and can be characterized based on their monosaccharide compositions estimated from their calculated molecular masses. Here, we study the glycosylation of Thy-1 by oligosaccharide profiling with GCC–LC/MS. First, we improved our oligosaccharide profiling by ion trap mass spectrometry (IT–MS) coupled with Fourier transform ion cyclotron resonance mass spectrometry (FT–ICR–MS). This instrument is capable of both monosaccharide composition analysis by acquisition of accurate masses and data-dependent multistage tandem MS ($MS^n$) for sequencing with fast switching between positive and negative ion modes. Using a mixture of typical oligosaccharides, including high-mannose-type, and asialo-, trisialylated, and tetrasialylated complex-types, we confirmed that the improved method can be used for monosaccharide composition analysis and detailed structural analysis of both neutral and acidic oligosaccharides. The method was then applied to N-linked oligosaccharide analysis of rat brain Thy-1.

## 2. Experimental

### 2.1. Materials

Man7/D1, Man7/D3, and asialo-triantennary (Tri) were obtained from Oxford Glycosystems (Abingdon, UK). Trisialylated triantennary ($TriNA_3$) and tetrasialylated tetraantennary ($TetraNA_4$) were purchased from Dionex (Sunnyvale, CA, USA). Rat brain was purchased from Nippon SLC (Hamamatsu, Japan). Phosphatidylinositol-specific phospholipase C (PIPLC) from *Bacillus cereus* was purchased from Molecular Probes (Eugene, OR, USA). Peptide-*N*-glycosidase F (PNGase F) was purchased from Roche Diagnostics (Mannheim, Germany). SimplyBlue SafeStain was obtained from Invitrogen (Carlsbad, CA, USA).

### 2.2. Release of N-linked oligosaccharides from rat brain Thy-1 by in-gel PNGase F digestion

PIPLC-treated GPI-anchored proteins were prepared from rat brain as reported previously [31]. Briefly, the homogenate of rat brain was defatted and solubilized with 2% Triton X-114 at 4 °C overnight [35,36]. After centrifugation, the supernatant was subjected to Triton X-114 phase-partitioning at 37 °C. Solubilized membrane proteins in the detergent phase were precipitated with cold acetone, and the precipitates were digested with PIPLC. After resubjecting the digest mixture to Triton X-114 phase-partitioning, PIPLC-treated soluble GPI-anchored proteins in aqueous phase were precipitated by adding cold acetone. These proteins were carboxyamidomethylated [30], and were separated by sodium dodecyl sulfate–polyacrylamide gel electrophoresis (SDS–PAGE) (12.5%) followed by staining with SimplyBlue SafeStain.

In-gel PNGase F digestion of Thy-1 and extraction of N-linked oligosaccharides were performed as previously described

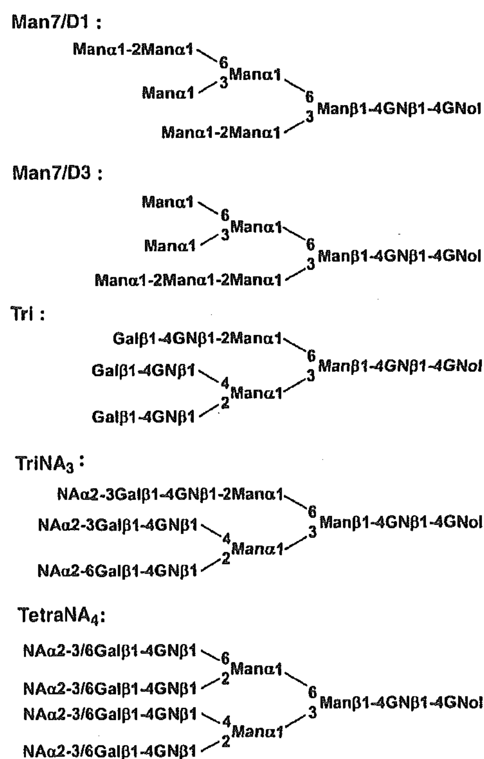


Fig. 1. Structures of major oligosaccharides and their abbreviations. Man: mannose, Gal: galactose, GN; *N*-acetylglucosamine, GNol; *N*-acetylglucosaminitol, NA; *N*-acetylneuramic acid.

[15]. The protein band of Thy-1 (20–25 kDa) was excised, cut into pieces, and destained. The gel pieces were dehydrated with 50% acetonitrile. The dried gels were then equilibrated with 50 mM sodium phosphate buffer (pH 7.2) and incubated at 37 °C with 3 units of PNGase F. The released *N*-glycans were extracted three times from gel pieces by intermittent sonication for 30 min in water. All extracts were combined and lyophilized. The released N-linked oligosaccharides were reduced with $NaBH_4$, as previously reported [33], and subjected to GCC–LC/IT–MS-FT–ICR–MS.

### 2.3. N-linked oligosaccharide analysis by GCC–LC/IT–MS-FT–ICR–MS

GCC–LC/MS was carried out using a MAGIC 2002 system (Michrom BioResource, Auburn, CA, USA) connected to IT–MS instrument coupled with FT–ICR–MS instrument (Finnigan LTQ FT, Thermo Electron Corp., San Jose, CA, USA). The eluents consisted of 5 mM ammonium acetate, pH 9.6, containing 2% $CH_3CN$ (pump A), and 5 mM ammonium acetate, pH 9.6, containing 80% $CH_3CN$ (pump B). The borohydride-reduced N-linked oligosaccharides were separated on Hypercarb (150 mm × 0.2 mm, 5 μm, Thermo Electron Corp.) as GCC with a linear gradient of 5–30% for pump B over a period of 60 min at a flow rate of 2 μl/min.

The $MS^n$ experiment includes sequential scans, as follows: a full $MS^1$ scan (*m/z* 700–2000) by FT–ICR–MS in positive ion mode, data-dependent $MS^n$ scans by IT–MS for most abundant ions regardless of their charge state, a full $MS^1$ scan (*m/z* 700–2000) by FT–ICR–MS in negative ion mode, and data-dependent $MS^n$ scans by IT–MS for the most intense ions regardless of their charge state. For the data-dependent $MS^n$, the following settings were used: the isolation window for precursor masses, ±2.5 Da; collision energy, 35%; dynamic exclusion

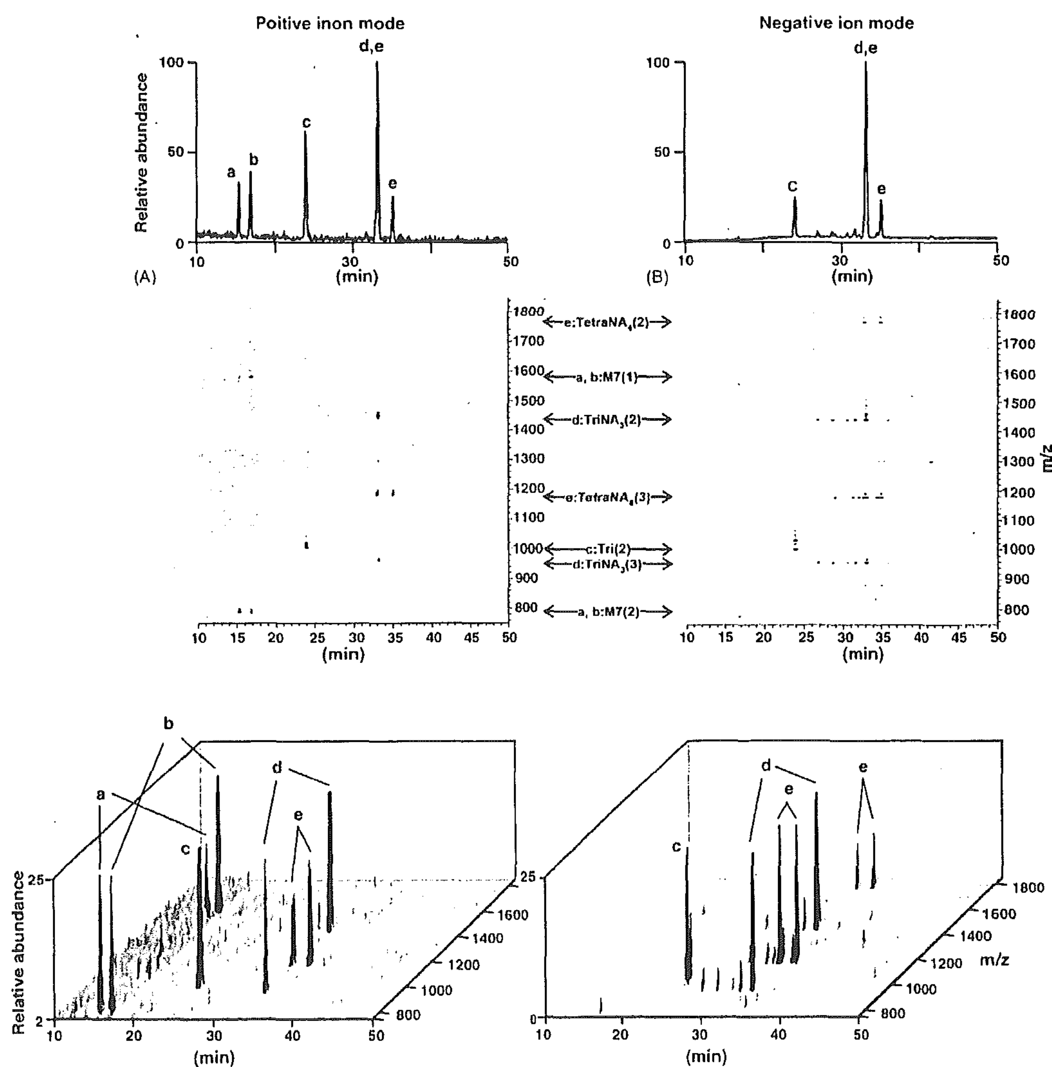


Fig. 2. Typical oligosaccharide profiles obtained by full $MS^1$ scans with FT–ICR–MS. (A) total ion chromatogram (TIC) (upper), two-dimensional (2D) display (retention time vs. *m/z*) (middle), and three-dimensional (3D) display (lower) in positive ion mode. (B) TIC (upper), 2D (middle) and 3D display (lower) in negative ion mode. Numbers in parentheses after the abbreviation of the model oligosaccharides refer to the charge state.

time, 15 s. The operating conditions employed for LC/MS$^n$ were as follows: tube lens offset, 120 V; capillary voltage, 2.0 kV; and capillary temperature, 200 °C.

## 3. Results

### 3.1. GCC–LC/IT–MS-FT–ICR–MS of model oligosaccharides

By using the IT–MS-FT–ICR–MS instrument, the oligosaccharide profiling was shown to be more rapid, accurate, and informative. Man7/D1, Man7/D3, Tri, TriNA$_3$, and TetraNA$_4$, which were chosen as model neutral and acidic oligosaccharides (Fig. 1), were analyzed by alternative scans in positive and negative ion modes, which are consisting of a full MS$^1$ scan by FT–ICR–MS followed by data-dependent MS$^n$ scans by IT–MS. Fig. 2A and B show the oligosaccharide profiles obtained by a full MS$^1$ scan with FT–ICR–MS (*m/z* 700–2000) in positive and negative ion modes, respectively. The monosaccharide compositions of individual oligosaccharides could be easily determined by accurate *m/z* values, and the major peaks of a, b, c, d, and e were assigned to Man7/D1 or D3, Man7/D3 or D1, Tri, TriNA$_3$ and TetraNA$_4$, respectively. Oligosaccharides detected at the same *m/z* values are positional isomers. Man7/D1 and D3 were detected in positive ion mode, but were only slightly detectable in negative ion mode. The major isomers of TriNA$_3$ and TetraNA$_4$ were detected in both ion modes, whereas their minor isomers were detected only in negative ion mode. These results demonstrate the advantage of alternative scans in both ion modes.

We confirmed the possibility of data-dependent MS$^n$ scans for sequencing neutral and sialylated oligosaccharides. Man 7/D1 and D3 could be distinguished from each other by data-dependent MS$^n$ (Fig. 3). Oligosaccharide eluted at 15 min could be assigned to Man7/D1 by the relatively intense ions at *m/z* 913 ($Y_{3\alpha}^+$) and 1237 ($Y_{3\beta}^+$), which would be predominantly produced from Man7/D1 by the cleavage of the α1–6-linked or α1–3-linked branch arm of the core mannose (Fig. 3A) (nomenclature proposed by Domon and Costello [37]). Likewise, the oligosaccharide at 17 min could be Man7/D3 based on the intensity of $Y_{3x}^+$ at *m/z* 1075 generated from Man7/D3 by the cleavages of both the α1–6-linked and α1–3-linked branch arms (Fig. 3B).

Fig. 4A and B show the product ion spectra of TetraNA$_4$ in positive and negative ion modes, respectively. In positive ion mode, the characteristic B ions such as *m/z* 454 ($B_{2x}^+$), 657 ($B_{3x}^+$), 1475 ($B_{4x}^+$), and 1658 ($B_6^{2+}$), and a ladder of several Y ions with intervals corresponding to Hex, HexNAc, and NeuAc were detected. B/Y ions were also detected at *m/z* 366, 527, 819 ($B_5/Y_{3x}^{2+}$), and 1330 ($B_6/Y_{4x}^{2+}$). In negative ion mode, only sialic acids were predominantly eliminated by MS$^2$ and MS$^3$. The structural information was provided by MS$^4$, whereby both B and Y ions were originated from TetraNA$_2$, together with the internal fragmentation ions and cross ring cleaved ions (Fig. 4B). In addition to the B and Y ions, which were predominantly produced in positive ion mode, fragment ions at *m/z* 470 ($C_{2x'}^-$), 1322 ($Z_{6x'}^{2-}$, $[Y_{6x'}\text{-}H_2O]^{2-}$), 1241 ($Z_{5x'}^{2-}$, $[Y_{5x'}\text{-}H_2O]^{2-}$), and 1057 ($Y_{5x''}/Z_{4x'}^{2-}$, $Y_{4x'}/Z_{5x''}^{2-}$, $Y_{4x''}/Z_{5x'}^{2-}$, $Y_{5x'}/Z_{4x''}^{2-}$, $[Y_{4x'/5x''}\text{-}H_2O]^{2-}$, $[Y_{4x''/5x'}\text{-}H_2O]^{2-}$) were detected in negative ion mode. These ions were also useful for the structural characterization of oligosaccharides.

### 3.2. Glycosylation analysis of Thy-1 by GCC-LC/IT-MS-FT-ICR–MS

The improved oligosaccharide profiling using IT–MS-FT–ICR–MS was applied to the glycosylation analysis of Thy-1. PIPLC-treated Thy-1 in rat brain was isolated by SDS–PAGE [31]. N-linked oligosaccharides were extracted from the gel after in-gel PNGase F digestion and were reduced

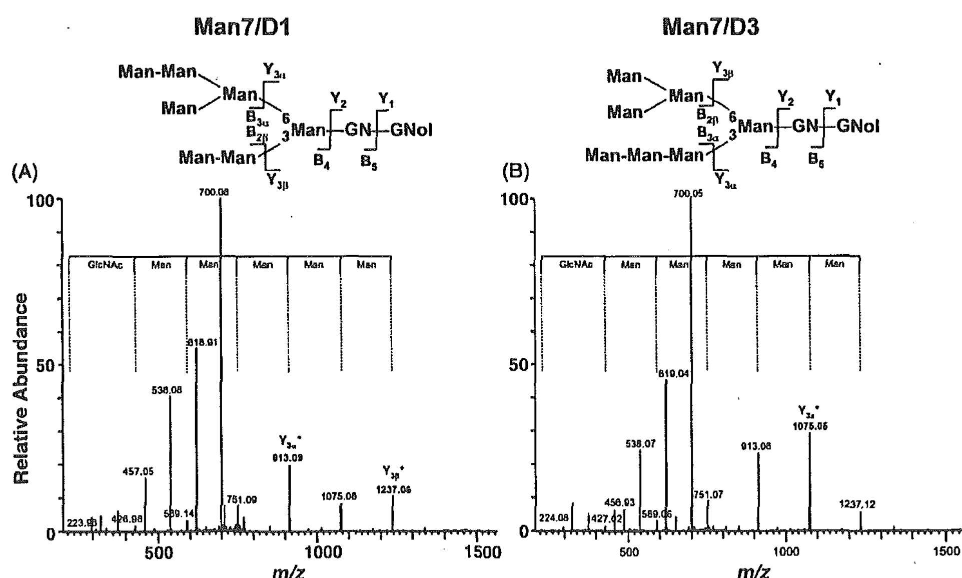


Fig. 3. Product ion spectra of oligosaccharide Man 7/D1 (A) and Man 7/D3 (B).

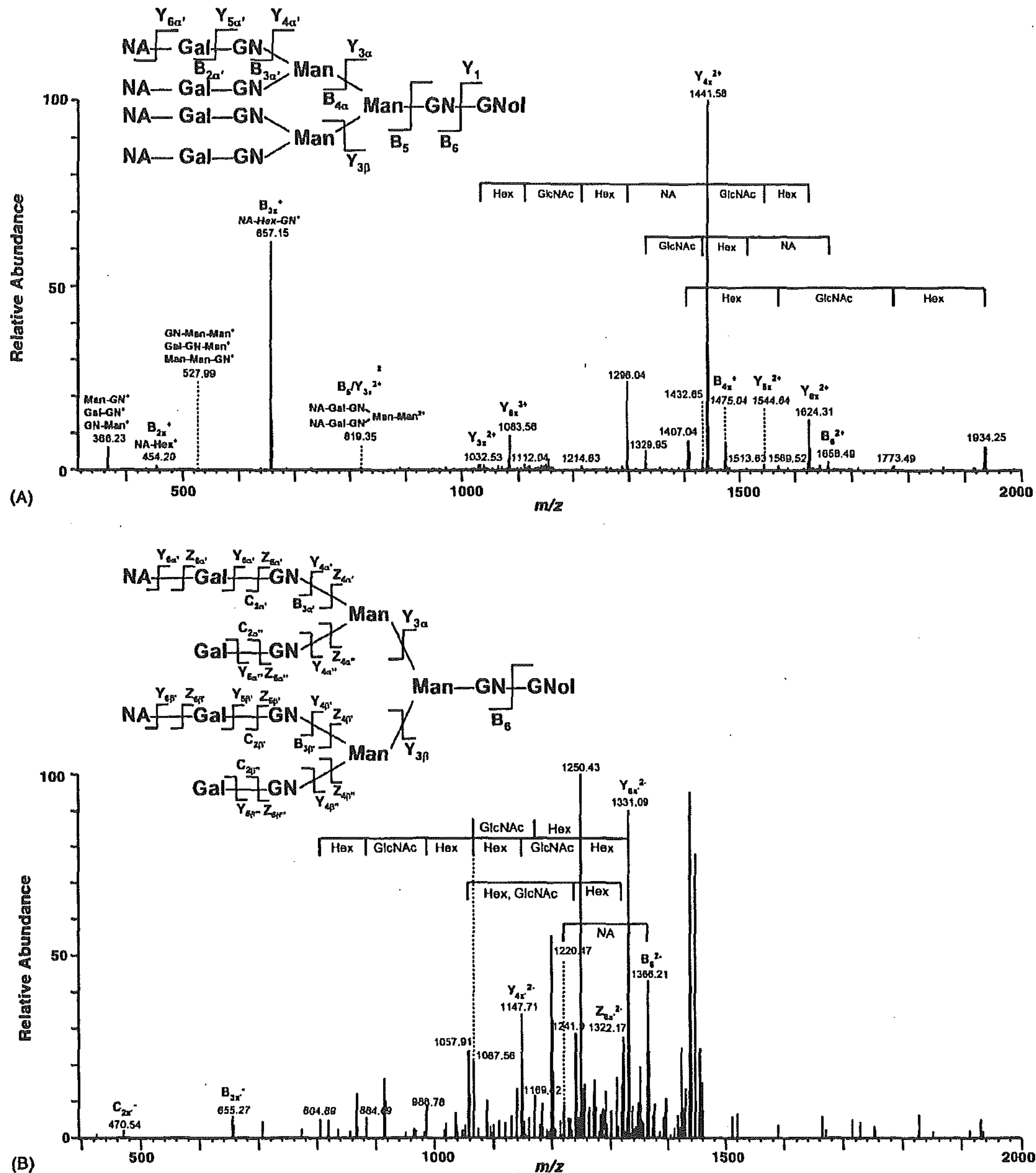


Fig. 4. Product ion spectra of model oligosaccharide, TetraNA$_4$. (A) MS$^2$ spectrum derived from $[\mathrm{TetraNA_4}]^{3+}$ at $m/z$ 1180 in positive ion mode. (B) MS$^4$ spectrum derived from $[\mathrm{TetraNA_4}]^{3-}$ at $m/z$ 1178 → $[\mathrm{TetraNA_3}]^{3-}$ at $m/z$ 1081 → $[\mathrm{TetraNA_2}]^{2-}$ at $m/z$ 1476 in negative ion mode.

with $NaBH_4$. Fig. 5 shows total ion chromatogram (TIC) (A) obtained by GCC–LC/IT–MS-FT–ICR–MS of borohydrate-reduced oligosaccharides, and two-dimensional display of full MS$^1$ scans in positive ion mode (red) and negative ion mode (blue) (B), in which oligosaccharides appear as protonated and ammonium adducted forms along with fragment ions. Alternative scanning in potitive and negative ion mode enables us to detect many oligosaccharides without missing less ionized oligosaccharides in either ion mode. For example, oligosaccharides at $m/z$ 762 (2+) and 822 (2+) were detected only in positive ion mode, whereas those at $m/z$ 1387 (2−), 1440 (2−), and 1542 (2−) were detected only in negative ion mode. Furthermore, accurate $m/z$ values acquired by FT–ICR–MS provide their monosaccharide composition, and subsequent data-dependent MS$^n$ allows us to elucidate their monosaccharide sequence as follows.

### 3.2.1. *Monosaccharide composition of oligosaccharides*

Oligosaccharides in Thy-1 were assigned to NeuAc$_{0-3}$ dHex$_{0-3}$Hex$_{3-9}$HexNAc$_{1-5}$HexNAcol$_1$ based on their accurate $m/z$ values (Table 1). Oligosaccharides bearing two Fuc residues, in which the $m/z$ values of multiple charged ions are nearly identical to those of oligosaccharides bearing one NeuAc residue instead, could be determined

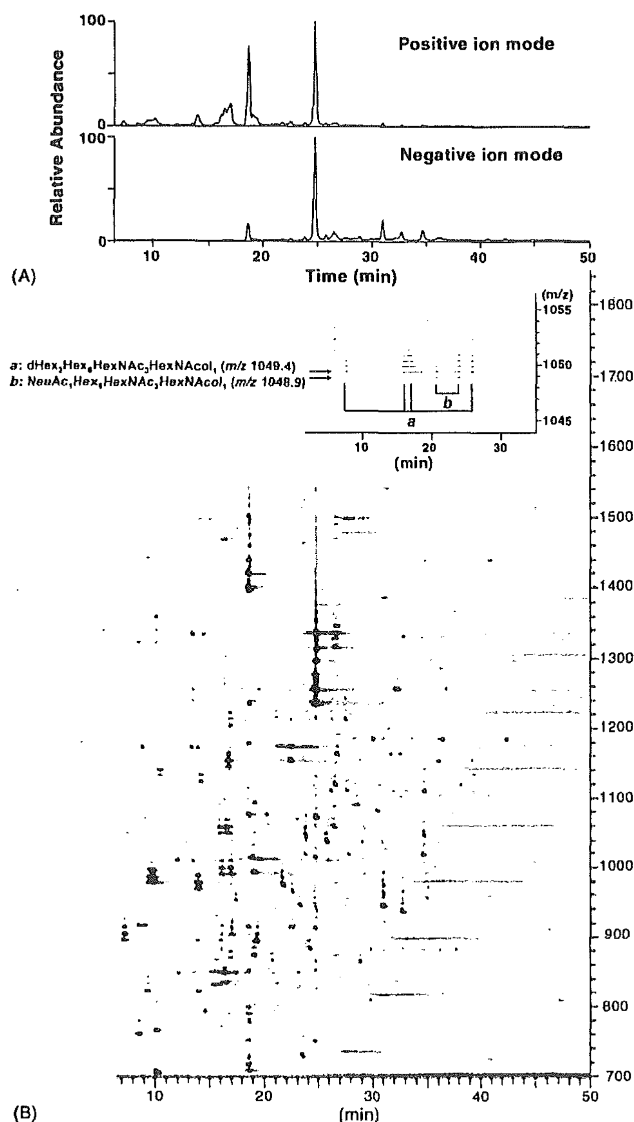


Fig. 5. N-Linked oligosaccharide profile of rat brain Thy-1 obtained by full MS[1] scans with FT–ICR–MS. (A) TIC, and (B) overlapped 2D display in positive (red) and negative (blue) ion modes.

by FT–ICR–MS. For instance, difucosylated oligosaccharides ($dHex_2Hex_6HexNAc_3HexNAcol_1$, theoretical molecular weight: 2096.78 Da) detected at 7.6, 16, 17, and 26 min (Fig. 5, inset, a) were clearly distinguished from monosialylated oligosaccharides ($NeuAc_1Hex_6HexNAc_3HexNAcol_1$, theoretical molecular weight: 2095.76 Da) detected at 21 and 24 min (Fig. 5, inset, b). The improved oligosaccharide profiling indicated that Thy-1 possesses a significant variety of N-linked oligosaccharides containing high-mannose-type (Man5, Man6, Man7, Man8, and M9) and many different complex- and hybrid-type oligosaccharides bearing $NeuAc_{0-3}$ and $Fuc_{0-3}$. These results are coincident with those of our previous study, in which we carried out mass spectrometric analysis of Thy-1 glycopeptides.

*3.2.2. Monosaccharide sequence of oligosaccharides*

Monosaccharide sequences of oligosaccharides were elucidated based on the MS/MS spectra. One of the remarkable features of Thy-1 oligosaccharides is the attachment of multiple Fuc and NeuAc residues. We describe below some examples of assignment fucosylated and sialylated oligosaccharides.

*3.2.2.1. Gal-(Fuc-)GlcNAc-(Lewis a/x type).* Fig. 6A shows the product ion spectrum of a difucosylated oligosaccharide, $dHex_2Hex_4HexNAc_3HexNAcol_1$, at *m/z* 887 (24.3 min) in positive ion mode. There are two possible sites of fucosylation: GlcNAc at the non-reducing end and at the reducing end in the trimannosyl core. The ions detected at *m/z* 350 (Fuc-GlcNAc$^+$, $B_{2\alpha}/Y_{5\alpha'}{}^+$), 370 (Fuc-GlcNAcol$^+$, $Y_{1\alpha}{}^+$), and 512 (Gal-(Fuc−)GlcNAc$^+$, $B_{2\alpha}{}^+$) indicate that Fuc residues link to both the non-reducing end like Lewis a/x, and the inner trimannosyl core GlcNAc. Other ions detected at *m/z* 1553 ($Z_{3\gamma}{}^+$, $[Y_{3\gamma}\text{-}H_2O]^+$) and 1570 ($Y_{3\gamma}{}^+$) suggest a linkage of non-substituted HexNAc at the terminal end. From these characteristic ions together with a Y ion at *m/z* 938.03 ($Y_{3\alpha/3\beta}{}^+$), it can be deduced that this HexNAc is a bisecting GlcNAc that attaches to the core mannose residue via β1–4 linkage. On the basis of these product ions, the oligosaccharide is assigned to the structure indicated in Fig. 6A, inset.

*3.2.2.2. Fuc-Gal-(Fuc−)GlcNAc−(Lewis b/y type).* Fig. 6B is the product ion spectrum of a difucosylated oligosaccharide, $dHex_2Hex_5HexNAc_4HexNAcol_1$, at *m/z* 1070 (9.2 min). The characteristic ions at *m/z* 512 (Gal-(Fuc−)GlcNAc$^+$, Fuc-Gal-GlcNAc$^+$, $B_{3\alpha'}/Y_{6\alpha'''}{}^+$, $B_{3\alpha'}/Y_{5\alpha''''}{}^+$) and 1915 ($B_6{}^+$) suggest the absence of Fuc at the reducing end GlcNAc; a B ion at *m/z* 658 ($B_{3\alpha'}{}^+$), a B/Y ion at *m/z* 350, and a Y ion at *m/z* 1408 ($Y_{3\beta/4\alpha''}{}^+$) suggest the attachment of two Fuc to Gal-GlcNAc at the non-reducing end, in a similar manner to the Lewis b/y antigen, Fuc-Gal-(Fuc−)GlcNAc−. A Y ion at *m/z* 1936 ($Y_{4\alpha''}{}^+$) indicates a linkage of non-substituted HexNAc at the terminal end. A B/Y ion at *m/z* 877 ($B_{4\alpha}/Y_{5\alpha''''}{}^+$, $B_{4\alpha}/Y_{6\alpha'''}{}^+$) and a Y ion at *m/z* 1610 ($Y_{3\beta}{}^+$) suggest that this non-substituted HexNAc residue is linked to the mannose residue attached to the Fuc-Gal-(Fuc−)GlcNAc− structure. These ions lead to assignment of this oligosaccharide as the structure indicated in Fig. 6B, inset.

*3.2.2.3. NeuAc-Gal-(NeuAc−)GlcNAc−.* Fig. 7A shows the product ion spectrum of a disialylated oligosaccharide, $NeuAc_2dHex_1Hex_5HexNAc_2HexNAcol_1$, at *m/z* 1085 (30.4 min). Characteristic fragment ions at *m/z* 495 ($B_{3\alpha}/Y_{5\alpha'}{}^+$), 948 ($B_{3\alpha}{}^+$), and 1110 ($B_{4\alpha}{}^+$), together with B ions at *m/z* 453 ($B_{2\alpha'}{}^+$) and 657 ($B_{3\alpha}/Y_{5\alpha''}{}^+$, $B_{3\alpha}/Y_{6\alpha'}{}^+$) suggest the presence of a partial structure of NeuAc-Gal-(NeuAc−)GlcNAc−. Furthermore, detection of Y ions at *m/z* 370 ($Y_{1\alpha}{}^+$) and 1059 ($Y_{3\alpha}{}^+$, $Y_{4\alpha/4\beta}{}^+$) as well as a B ion at *m/z* 1799 ($B_6{}^+$) indicate the linkage of a Fuc residue at the inner trimannosyl core GlcNAc. Based on these product ions, the oligosaccharide detected at *m/z* 1085 was assigned to the structure in Fig. 7A, inset.

Table 1
Summary of N-linked oligosaccharides of rat brain Thy-1

| Monosacchardic composition[a] | | | | Theoretical mass[b] | Positive ion mode | | Negative ion mnmode | | Deduced structure[d] |
|---|---|---|---|---|---|---|---|---|---|
| dHex | Hex | HX | NA | | Observed $m/z$[c] | Retention time (min) | Observed $m/z$[c] | Retention time (min) | |
| 1 | 3 | 2 | 0 | 1058.40 | 1059.46(1) | 29.17 | | | CoreF |
| 0 | 5 | 2 | 0 | 1236.45 | 1237.47(1) | 24.74 | 1235.45(1) | 24.76 | M5 |
| 0 | 3 | 4 | 0 | 1318.50 | 1319.57(1) | 8.63 | | | |
| 0 | 6 | 2 | 0 | 1398.50 | 1399.53(1) | 18.73 | 1397.50(1) | 18.68 | M6 |
| 0 | 5 | 3 | 0 | 1439.53 | 1440.59(1) | 9.17 | | | |
| 1 | 3 | 4 | 0 | 1464.56 | 733.31(2), 1465.65(1) | 23.44 | | | |
| 0 | 3 | 5 | 0 | 1521.58 | 761.80(2) | 8.63 | | | BisectGN |
| 0 | 7 | 2 | 0 | 1560.55 | 781.29(2), 1561.60(1) | 18.66 | | | M7 |
| 1 | 5 | 3 | 0 | 1585.59 | 793.82(2) | 14.59 | | | Hybrid |
| 1 | 5 | 3 | 0 | 1585.59 | 793.81(2) | 19.13 | | | |
| 1 | 5 | 3 | 0 | 1585.59 | 793.83(2) | 20.96 | | | |
| 0 | 5 | 4 | 0 | 1642.61 | 822.33(2) | 9.48 | | | Hybrid |
| 0 | 5 | 4 | 0 | 1642.61 | 822.33(2) | 14.02 | | | |
| 1 | 3 | 5 | 0 | 1667.64 | 834.83(2), 1668.69(1) | 16.48 | 832.81(2) | 16.44 | CoreF |
| 0 | 4 | 5 | 0 | 1683.63 | 842.85(2) | 17.48 | | | Hybrid |
| 0 | 8 | 2 | 0 | 1722.61 | 870.83(2)[e] | 17.07 | | | M8 |
| 0 | 5 | 3 | 1 | 1730.62 | 866.34(2) | 20.31 | | | |
| 0 | 5 | 3 | 1 | 1730.62 | 866.35(2) | 28.91 | 864.31(2), 1729.64(1) | 28.93 | Hybrid |
| 2 | 5 | 3 | 0 | 1731.64 | 866.86(2) | 20.83 | 864.81(2) | 20.85 | Hybrid, CoreF, Lax |
| 1 | 6 | 3 | 0 | 1747.64 | 874.84(2) | 19.19 | | | |
| 2 | 4 | 4 | 0 | 1772.67 | 887.37(2) | 23.84 | 885.33(2) | 23.86 | |
| 2 | 4 | 4 | 0 | 1772.67 | 887.36(2) | 24.25 | 885.33(2) | 24.27 | Hybrid, CoreF, BisectGN |
| 1 | 5 | 4 | 0 | 1788.67 | 895.36(2) | 7.37 | | | Hybrid |
| 1 | 5 | 4 | 0 | 1788.67 | 895.36(2) | 13.90 | | | |
| 1 | 5 | 4 | 0 | 1788.67 | 895.35(2) | 14.16 | | | Hybrid, CoreF |
| 1 | 5 | 4 | 0 | 1788.67 | 895.35(2) | 19.44 | 893.33(2) | 19.46 | Hybrid, CoreF |
| 0 | 6 | 4 | 0 | 1804.66 | 903.35(2) | 17.07 | 901.33(2) | 17.09 | Hybrid, BisectGN |
| 1 | 4 | 5 | 0 | 1829.69 | 915.88(2) | 8.63 | | | Hybrid |
| 1 | 4 | 5 | 0 | 1829.69 | 915.88(2) | 9.17 | | | Hybrid |
| 1 | 4 | 5 | 0 | 1829.69 | 915.89(2) | 18.00 | | | Hybrid |
| 1 | 4 | 5 | 0 | 1829.69 | 915.89(2) | 22.61 | 913.84(2) | 22.63 | |
| 1 | 5 | 3 | 1 | 1876.68 | 939.37(2) | 21.17 | 937.34(2) | 21.12 | |
| 1 | 5 | 3 | 1 | 1876.68 | 939.36(2) | 24.90 | 937.34(2) | 24.92 | |
| 1 | 5 | 3 | 1 | 1876.68 | 939.39(2) | 32.76 | 937.33(2) | 32.78 | Hybrid, CoreF |
| 0 | 9 | 2 | 0 | 1884.66 | 951.88(2)[e] | 17.53 | | | M9 |
| 0 | 6 | 3 | 1 | 1892.68 | 947.39(2) | 23.31 | 945.33(2) | 23.33 | Hybrid |
| 0 | 6 | 3 | 1 | 1892.68 | 947.39(2) | 31.09 | 945.33(2) | 31.05 | Hybrid |
| 2 | 6 | 3 | 0 | 1893.70 | 947.87(2) | 24.61 | 945.84(2) | 24.70 | |
| 1 | 4 | 4 | 1 | 1917.71 | | | 957.85(2) | 27.73 | |
| 1 | 4 | 4 | 1 | 1917.71 | | | 957.85(2) | 28.86 | |
| 1 | 4 | 4 | 1 | 1917.71 | | | 957.85(2) | 34.91 | CoreF |
| 1 | 4 | 4 | 1 | 1917.71 | | | 957.85(2) | 35.55 | |
| 0 | 5 | 4 | 1 | 1933.70 | 967.89(2) | 22.61 | 965.85(2) | 22.63 | Hybrid |
| 0 | 5 | 4 | 1 | 1933.70 | 967.86(2) | 24.61 | 965.82(2) | 24.70 | |
| 2 | 5 | 4 | 0 | 1934.72 | 968.39(2) | 13.97 | | | Hybrid |
| 1 | 6 | 4 | 0 | 1950.72 | 976.39(2) | 9.93 | | | Hybrid, Lax |
| 1 | 6 | 4 | 0 | 1950.72 | 976.41(2) | 21.76 | 974.35(2) | 21.79 | Hybrid, CoreF |
| 2 | 4 | 5 | 0 | 1975.75 | 988.90(2) | 16.21 | 986.85(2) | 16.16 | Complex |
| 2 | 4 | 5 | 0 | 1975.75 | 988.90(2) | 17.07 | 986.87(2) | 17.09 | Complex |
| 0 | 5 | 3 | 2 | 2021.72 | | | 1009.86(2) | 26.35 | |
| 0 | 5 | 3 | 2 | 2021.72 | | | 1009.85(2) | 26.83 | |
| 1 | 6 | 3 | 1 | 2038.73 | 1020.40(2) | 23.84 | 1018.36(2) | 23.80 | |
| 1 | 6 | 3 | 1 | 2038.73 | 1020.44(2) | 27.77 | 1018.37(2) | 27.80 | CoreF |
| 1 | 6 | 3 | 1 | 2038.73 | 1020.42(2) | 34.66 | 1018.36(2) | 34.69 | Hybrid, CoreF |
| 1 | 5 | 4 | 1 | 2079.76 | 1040.92(2) | 25.73 | 1038.87(2) | 25.81 | CoreF |
| 1 | 5 | 4 | 1 | 2079.76 | 1040.92(2) | 29.04 | 1038.88(2) | 28.99 | |
| 3 | 5 | 4 | 0 | 2080.78 | 1041.42(2) | 23.84 | 1039.39(2) | 23.86 | |
| 0 | 6 | 4 | 1 | 2095.76 | 1048.94(2) | 20.57 | | | Hybrid |
| 0 | 6 | 4 | 1 | 2095.76 | 1048.91(2) | 23.84 | 1046.87(2) | 23.80 | Hybrid |
| 2 | 6 | 4 | 0 | 2096.78 | 1049.42(2) | 7.58 | | | |